Questions for the test-hall walkthrough

16.10.2023

- What is the difference between **ADS.fAHURHTempSupPrimADS** and **ADS.fAHURHTempSupADS** datapoints? (what does **Prim** mean?)

- What measurement/metric **ADS.bAHUCOPumpOperatingADS** datapoint track?

- What is the purpose of the **Exhaust Air** pipeline? → is it to exhaust out air when the inside air temperature is too hot?

- What is the meaning of the **fAHUHRBypValveAct1ADS** datapoint? How does the 'bypass valve' work in the **Heat Recovery**?
    - Both the actual valve (fAHUHRBypValveAct1ADS) and the setpoint valve (fAHUHRBypValveSetADS) time series values are between 0 and 100. What does this signify?

- What is the function of the **Heat Recovery**, in relation to the Extract and Supply Air?

- The **cooler** and **reheater** (both situated within the Supply Air pipeline) have opposite functions (as per my assumption). Therefore, are they both on at the same time?

I have added a few more questions as comments in the Schraven et al. paper (attached below) on pages 8-10 of this PDF.

RWTH-EBC 2023-001

A comprehensive building HVAC design for application of model-predictive control: Experiences and challenges of construction, commissioning, and operation in a real-world scenario

Markus Hans Schraven[1,*], Marc Axel Baranski[2], Alexander Kümpel[1], Dirk Müller[1]

[1] RWTH Aachen University, Institute for Energy Efficient Buildings and Indoor Climate, Mathieustraße 10, 52074 Aachen, Germany
[2] aedifion GmbH, Hohenzollernring 72, 50672 Cologne, Germany
[*] Correspondence: mschraven@eonerc.rwth-aachen.de; Tel.: +49-241-80-49592

Please cite this article as:

M. H. Schraven, M. A. Baranski, A. Kümpel, D. Müller, *A comprehensive building HVAC design for application of model-predictive control: Experiences and challenges of construction, commissioning, and operation in a real-world scenario*, In: RWTH Publications, White Paper RWTH-EBC 2023-001, Aachen, 2023, DOI: 10.18154/RWTH-2023-03811

RWTH Aachen University
E.ON Energy Research Center
Institute for Energy Efficient Buildings and Indoor Climate (EBC)
Mathieustr. 10, 52074 Aachen

T +49 241 80-49760, F +49 241 80-49769
ebc-office@eonerc.rwth-aachen.de, www.eonerc.rwth-aachen.de/ebc

A comprehensive building HVAC design for application of model-predictive control: Experiences and challenges of construction, commissioning, and operation in a real-world scenario

Markus Hans Schraven[1,*], Marc Axel Baranski[2], Alexander Kümpel[1], Dirk Müller[1]

[1]*RWTH Aachen University, Institute for Energy Efficient Buildings and Indoor Climate, Mathieustraße 10, 52074 Aachen, Germany*
[2]*aedifion GmbH, Hohenzollernring 72, 50672 Cologne, Germany*
[*]*Correspondence: mschraven@eonerc.rwth-aachen.de; Tel.: +49-241-80-49592*

Abstract
Building energy systems (BES) and in particular heating, ventilation and air conditioning (HVAC) systems are a major source of greenhouse gas emissions. Many studies have addressed the multi-criteria problem of energy efficiency, comfort, and control in HVAC systems, one of the most popular approaches in academic research being model-predictive control (MPC). However, just 21 % of these approaches are validated in practical applications. Especially the overall construction, commissioning, and operation process is rarely considered, despite affecting the integration of MPC significantly. The objective of this article is three-fold: First, to close a gap in building HVAC description of real-world examples, a comprehensive documentation of a real-world HVAC system, related subsystems, and the control system is presented, including planning documents such as heating and cooling schemes, a control schema, and a building information model (BIM). In this particular case, the authors were involved in the building construction process of an industrial hall and its technical building equipment. Therefore, the second contribution is to share the experiences and a design of HVAC and control system. Finally, as the intended application is to research MPC performance, an MPC was implemented alongside the basic control. After tackling the major issues, the model used in the MPC was tuned and validated with measurement data, resulting in a root mean square error of 0.59 K for the approximated hall temperature. In a simulation experiment, the MPC saves 12 % of the end energy compared to a benchmark scenario.

Keywords
building energy systems (BES); heating, ventilation and air conditioning (HVAC); building automation and control systems (BACS); model-predictive control (MPC); building information modeling (BIM)

Contents

1 Introduction

The building sector is responsible for 36 % of the global final energy use and nearly 40 % of the energy-related carbon dioxide emissions [1]. A large proportion of the energy use arises from building energy system (BES), roughly 40 % to 70 % in particular from heating, ventilation and air conditioning (HVAC) systems [2], which are designed to provide users a comfortable environment and have experienced increasing application in the last few years [3, 4]. BES and HVAC operation optimization is a multidimensional problem including energy consumption, comfort, and control requirements, and has been addressed

by many researchers in the past. For instance, Halhoul Merabet et al. [5] as well as Shaikh et al. [6] present a review of different controls for energy and comfort management, Chua et al. [7] present a review of technologies and strategies for achieving an energy-efficient air conditioning. A recent article by Mariano-Hernández et al. summarizes strategies for building energy management systems [8]. While proportional-integral-derivative (PID) control is still the most commonly used control type overall [9, 10], research in HVAC operation is increasingly directed towards model-predictive control (MPC) [8, 11, 12].

For instance, in [13], Morosan et al. propose a distributed MPC and apply it to a thermal building simulation model. Compared to a PID reference control, their MPC generated savings of 25 % at comparable thermal comfort. Manjarres et al. report a 48 % heating and 39 % cooling consumption reduction for the HVAC system in a simulated office building [14]. Bianchini et al. apply an economic MPC to a system comprising HVAC, photovoltaic and storage devices [12]. For the simulated office building, in comparison to a thermostatic controller as a reference, their MPC yielded 25 % fewer costs. In [15], Sangi proposes a multi-agent MPC and applies it to a simulation model of a BES comprising a boiler, a combined heat and power unit, a heat pump as well as an electrical back-up heater. The performance is barely improved by 0.7 % compared to the PID- and mode-based reference control. Especially during the last years, artificial intelligent-based control approaches have been studied in literature. For instance, Kathirgamanathan et al. provides a review of data-driven MPC and future trends [16], Schreiber et al. implement a reinforcement learning control to a cooling supply system [17] and Anastasiadi et al. develop a fuzzy logic controller for HVAC systems and test it in a simulation framework [18]. Further, Stoffel et al. investigate different machine-learning based control approaches for room temperature control [19]. A simulation study showed that the considered approaches can outperform a rule-based control and the potentials and challenges for algorithm is discussed.

While numerous simulation studies exist, application examples and the challenges of real-life implementations are rarely investigated [20]. In this regard, Killian and Kozek present ten related questions to be considered when applying an MPC to a real building [20]. In fact, according to Serale, merely 21 % of the MPC-related scientific literature include experimental case studies [21], thus many approaches still require practical evaluation. Application examples include, among others, the following: Zacekova et al. show an application in an office building with a thermally active building system (TABS) and air handling unit (AHU) and identify the system identification process as a major issue [22]. They report an energy consumption reduction of 17 % compared to the original control strategy. Sangi et al. [23] use an exergy-based MPC to control a heat exchanger system, which outperforms the original implemented control of the heat exchanger system. In [24], Lindelöf et al. give an overview of successful application examples for MPC in HVAC systems and present their own adaptive MPC for heating control in ten test sites of residential buildings. Cai et al. [25] offer two case studies - a chiller plant control and a centralized air conditioning system serving a multi-zone building - to their multi-agent approach. In the second case study, savings amounted to 42.7 %. Coninck and Helsen propose an MPC framework and apply this to an office building including fan coil units, radiators and an AHU revealing cost savings between 34 % to 40 % over the rule-based reference control [26].

However, in real applications, even more than in the simulation studies, the reference buildings are very individual and no standard benchmark energy system model or control is used. The results are thus hardly comparable [27], especially since the majority of research does not take all expenses into account. For instance, further shortcomings concerning real applications arise from model deviations due to faults in design or devices, unconsidered states, or changes

in operation [22, 24] so that an effort-intensive, accurate, and usually system-specific modeling is required. Da Silva et al. conclude that, given low MPC model quality, a PID still outperforms an MPC and is more suitable for robust solutions due to lower complexity [28]. Sturzenegger et al. find that savings in operational expenses are often compensated by the additional required engineering, commissioning, and hardware for an MPC implementation, which do not justify the implementation effort in the end [29]. According to Cheng and Lee, artificial-intelligence-based control faces similar issues [30]. Hence, Killian et al. estimate the largest challenges to be the required expertise and risk responsibility when implementing a sophisticated MPC and integrating it into the automation infrastructure [20].

While comfort is often just a boundary condition, evaluation of energy efficiency seems fairly easy compared to control - which has to take control deviations but also vague influencing factors like the implementation effort or component strain due to switching operations into account - however, predictions of operational benefits are generally often overestimated. In fact, in this context, the gap between predicted and measured energy performance has recently become more visible due to the progressive deployment of monitoring systems and has been stressed, for example, by Wilde [31] or Shi et al. [32]. Wilde groups mismatch causes into three stages, namely design, construction, and operation, and specifies individual aspects in each stage [31]. Shi et al. present a literature overview on the performance gap and address five key questions: definition, magnitude, causes, determination, and solutions [32]. In [33], Eon et al. specifically focus on the construction and commissioning stage since it is rarely considered [34] but equally responsible for energy performance gaps as the other stages. They identify, among others, a lack of knowledge and skill as one major issue [33]. Another review of gray literature case studies points out user guidance and manufacturer standards as an important aspect [35]. Concrete investigations related to the energy impacts of typical design and operation faults in air conditioning systems have been conducted in a simulation study by Lee et al. [36]. Fahim et al. show performance increases of 15 % by addressing very simple issues like simultaneous heating and cooling and calibration of thermostats [37], which shows the benefits of early detection and solution of faults [38].

Considering this state of research, a significant lack in the investigation of practical MPC applications in HVAC systems is identified. This specifically includes the comparison with a reference control, which, as discussed in [21], may only be available in retrofitting cases. Targeting this gap, an MPC and an additional baseline control are developed for an industrial hall BES. Furthermore, the literature on the energy performance gap suggests a lack of a well-structured commissioning process and knowledge about common issues in practical HVAC applications. Consequently, in this paper, we contribute to the scientific literature on the energetic performance of buildings by discussing practical challenges that limit performance and hinder optimization measures. A major contribution is the comprehensive building HVAC and measurement and control technology (MCT) description supported by supplementary material covering heating and cooling schemes, a list of all devices (e.g. sensors and actuators) as well as a building information model (BIM) of the complete system allowing readers to directly use the information for calibrating their own MPC models or further applications. The discussion of challenges includes practical examples that show how high performance can be achieved. The main groups of challenges addressed are construction and operation faults on the one hand and, on the other hand, the challenges of the practical implementation of MPC in BES and in particular HVAC systems.

The method to identify the challenges is an in-depth study of a real-life BES. The BES is a newly-built experimental hall of the E.ON Energy Research Center (E.ON ERC) in Aachen. Through our deep involvement in planning, construction,

and commissioning, we could experience various issues entailing performance losses. Being responsible for the HVAC system construction and the MCT trade, we could additionally influence the interfaces to various devices and fit communication to our needs. Communication tends to remain one of the major challenges in building automation and control system (BACS) due to the heterogeneity of interfaces and protocols [39]. Moreover, we designed, commissioned, and improved the BACS in such a way that we achieved a reliable automation system that can be extended with a supervisory MPC to achieve optimization.

The rest of this paper is structured as follows: First, in section 2, the energy system of the experimental hall is presented. To showcase the functionality and usability, this section additionally covers a PID-based example control and a simplified MPC to be compared in a case study. In section 3, the experienced issues are discussed and the two control strategies are compared and evaluated. Section 4 summarizes the results and concludes this work. For better comprehensibility of the design decisions, a list of all devices and data points along with the MCT scheme and the BIM is openly available in the supplementary material at https://github.com/RWTH-EBC/EBC-SupplementaryMaterials (see section 4 for a full list of supplementary materials).

2 Methodology

The following sections cover an overview of the BES, MCT-related information and the applied control routines in the case study as well as measures taken to check the functionality and solve detected issues.

2.1 Building Description and Energy System

2.1.1 Building Description

The investigated BES is part of a recently constructed industrial hall located in Aachen, Germany. The construction process of the building and the technical building equipment finished at the end of 2018. The industrial hall is divided into 3 areas, subsequently referred to as hall 2, hall 1, and the office area. Floor areas amount to roughly $380\,m^2$ for hall 2 and $630\,m^2$ for hall 1. In these areas, the room height accounts for 7.4 m. The office area comprises two conference rooms with floor areas of about $19\,m^2$ each, two office rooms with floor areas of about $19\,m^2$ as well, a workshop room with a floor area of $17\,m^2$, two bathrooms with a combined floor area of around $9\,m^2$, a kitchen area with $6\,m^2$ floor area, battery room and the central fire alarm system with a total floor area of $4\,m^2$ and a corridor with approximately $28\,m^2$. Hence, the total office area amounts to roughly $140\,m^2$. The building has no basement, the technical building equipment is mostly located on top of the office area. Hence, in the office area, the headroom accounts for about 3 m while it amounts to approximately 4.2 m in the technical area above. In hall 1, only the emergency doors offer small viewing windows. The exterior facade consists of cassettes with integrated insulation and a heat transfer coefficient $<40\,W/(m^2\,K)$. A rough estimation of about $1250\,m^2$ can be given for the total area of the exterior walls. The roof area is approximate $1175\,m^2$. In the office area, the office, workshop, and meeting rooms as well as the corridor have double-glazed windows with a heat transfer coefficient of $1.1\,W/(m^2\,K)$ and a total window area of roughly $26\,m^2$.

For the planning of the placement of plants, air ducts, and piping system, the BIM tool mh-software [40] was used. In addition to a separation by trades contriving different models for air ducts and hydraulic piping, these models have been divided further, e. g. according to the floor or different construction phases. The integrated floor plan and models are provided in the supplementary material.

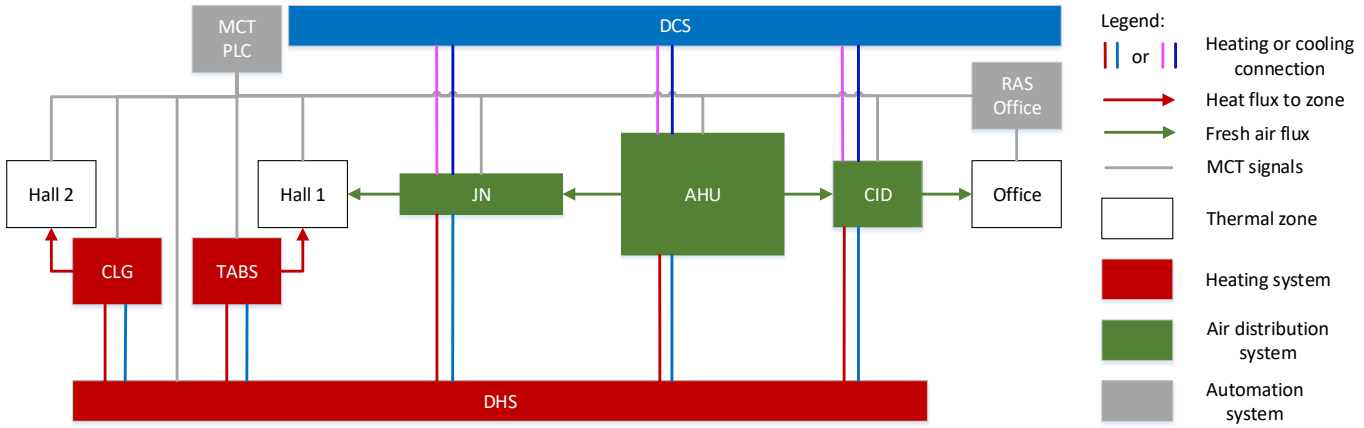

Figure 1 – System diagram of the building energy system. The detailed description and explanation of abbreviations are given in section 2.1.2

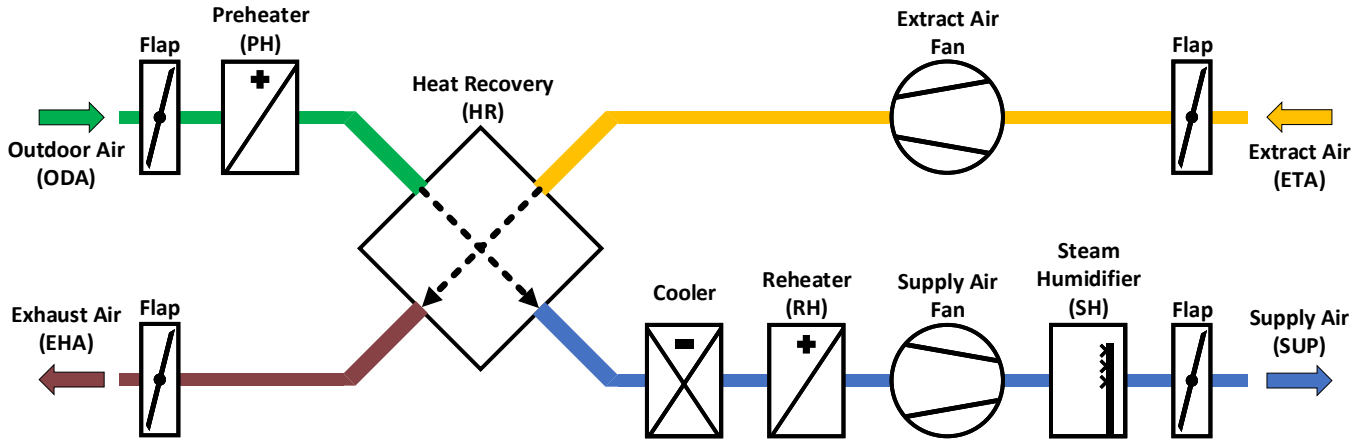

Figure 2 – Schematic view of the air handling unit.

2.1.2 Energy System

The energy system of the industrial hall consists of a central heat distributor, which is fed by a district heating station (DHS) and by analogy a cooling distributor, which is fed by a district cooling station (DCS)[1]. Electricity demand is supplied through the electrical grid. From the heat distributor, heat is supplied to hall 2 by ceiling panel heaters (CLGs), to hall 1 by a TABS as well as an AHU and decentralized heat exchangers, and to the office area via the supply air (SUP) through ceiling induction diffusors (CIDs). Similarly, from the cooling distributor, cold water is supplied to the AHU cooler, the CIDs, and the decentralized heat exchangers in hall 1. They are located in the SUP before jet nozzles (JNs) which distribute the conditioned air provided by a central AHU. The extract air (ETA) in hall 1 is collected centrally in the proximity of the AHU. Due to acoustic requirements, hall 2 has no mechanical ventilation but is rather ventilated via an $8.4\,\mathrm{m} \times 0.8\,\mathrm{m}$ ventilation grille. Figure 1 and 2 show a schematic view of the energy system and the air treatment options given by the AHU.

As the system integration of the DCS has not been completed, yet, the control of the related cooling systems has mostly been omitted in the subsequent sections.

The heating and cooling power of each system along with their temperature design points are summarized in table 1. For Aachen, heating systems are related to a design point of $-12\,^{\circ}\mathrm{C}$ in

[1] Note that the BIM contains two DCS, where only one of them is responsible for the BES supply.

winter, cooling systems to 32 °C ambient air temperature in summer, respectively.

2.2 Measuring and Control Technology

The BACS comprises a programmable logic controller (PLC) as a central element of the MCT system as well as a room automation system (RAS) with individual controllers for each room, incorporating the corresponding peripherals. Two cabinets - one for the MCT components and one for the AHU - include almost all of the required electrical components like controllers, terminals, power supply, network switches, and protocol routers. The central PLC is an industrial personal computer (IPC) from Beckhoff® and located in the MCT cabinet. A direct digital controller (DDC) is often specified by a fixed number of inputs and outputs, which makes them well-designed for preconfigured plants. With the different parts of the BACS being installed incrementally and without knowing the exact devices and interfaces beforehand, we chose to use a PLC over DDC due to its higher flexibility. The Beckhoff® PLC offers terminals for the communication with field devices like EL3214 for collecting data from PT100 temperature elements or EL4008 for providing 0–10 V signals for single-ended transmission to an actuator. In general, each company's automation controller brings its own software [41]. For Beckhoff®, the TwinCAT® software is used for programming, however, all open language implementations according to the IEC 61131 are supported. Since the distance to components in hall 2 is rather large, a decentralized field bus controller is mounted in a small cabinet within hall 2 to interface these components. This controller is directly connected to the central PLC. In addition, five zone controllers interface the devices within the office rooms. They are connected in series with the last module interfacing the central PLC again. The AHU was delivered with an individual AHU cabinet and controller, which is connected to the central PLC as well.

For detailed information on the MCT hardware, the MCT schema and a complete list of devices and data points are provided in the supplementary material.

2.3 System Integration

Communication in BACS requires components to support interoperable communication interfaces. Even though for this exact reason, the BACnet® standard has been introduced with ISO 16484-5, due to the fragmented building construction process, bidders of a tender seldom offer components with compatible communication interfaces as their focus rather lays on costs or they do not have interoperable devices in their portfolio [42]. Speaking of costs, usage of a bus protocol interface like BACnet® makes sense, especially for complex components with multiple sensor data or data points included such as DDCs of plants, pump control interfaces, or volume flow controllers. Valve actuators, however, that only drive a spindle to a certain set position and return a feedback signal, are not as complex and therefore would not benefit much from using the BACnet® protocol. Hence, these components are usually designed with simple analog 0–10 VDC signals.

While it is desirable to use as few different interfaces as possible, due to project requirements[2], the volume flow controllers in hall 1 are specified with Modbus® RTU. This applies to the room controllers as well, that interface the respective components within the rooms via MP-Bus. The master controller of the RAS, however, connects to the MCT PLC via BACnet® IP. The hydraulic pumps are connected in a BACnet® MS/TP network and via a BACnet® MS/TP to IP gateway to the MCT PLC. For 0–10 V components with a long distance transmission path (>40 m), the signal is converted to 0–20 mA directly at the device to avoid high voltage drops. All temperature elements are designed as passive 3-wire PT100 elements with 1/3 DIN accuracy. Compared to standard 2-wire temperature probes, the 3rd wire is used to form an additional measurement circuit

[2] The project partner developed radio-based communication interfaces for Modbus® RTU components.

Table 1 – Overview of heating and cooling design points. For details refer to the heating and cooling schemes in the supplementary material.

Device	Power	Design point primary	secondary
District heating station	270 kW	130/55 °C	80/50 °C
District cooling station	200 kW	7/15 °C	10/18 °C
		distributor	consumer
Thermally active building system	55 kW	80/50 °C	50/40 °C
Ceiling panel heaters	30 kW	80/50 °C	70/50 °C
Ceiling induction diffusers (5x)	1 kW each cooling 1.5 kW each heating	10/18 °C 80/50 °C	12/18 °C, T_R = 24 °C 50/30 °C, T_R = 20 °C
Air handling unit	63.1 kW preheater 149 kW cooler 56.7 kW reheater	80/50 °C 10/18 °C 80/50 °C	70/50 °C 10/18 °C 55/45 °C
Reheater/Recooler jet nozzles (2x)	20 kW each heating 12 kW each cooling	80/50 °C 10/18 °C	50/40 °C, m = 1750 kg/h 12/18 °C, m = 1750 kg/h

compensating the wire resistance and hence enhancing measurement accuracy. For a full specification of all components, we refer to the list of devices in the supplementary material.

2.4 Case Study - Control Routines

To demonstrate the functionality and usability of the proposed system, a case study is conducted comparing a PID-based example control with a simplified supervisory MPC. More specifically, the automation program that we implemented offers a mode-based control where the local auto mode represents our baseline control (see subsequent section 2.4.1), which mainly features simple PID control and heating curves along with some energy balances for the AHU control. The TwinCAT® the software supports communication with external devices via an automation device specification (ADS) interface. Hence, another mode is arranged for external control that enables direct access to each data point of the field devices from an external algorithm via ADS. For each plant, it is possible to switch the operation between the local and external control, which offers a flexible solution to add a supervisory control without compromising the baseline control.

Figure 3 summarizes the layout for the considered case study. The subsequent sections cover the control routines used in the case study.

2.4.1 PID-based Example Control

Heat Supply and Distribution To determine the required temperature on the heat distributor, the BACS collects all supply water temperature set points and adds a margin of 10 K to the maximum required temperature. In our experience, this margin sufficiently compensates heat flux losses on heat exchangers and improves part load behavior to a certain degree. This temperature set point is then set for the DHS[3]. On the DDC of the DHS, a PID control supplies two valves to adjust the power according to the required temperature on the secondary side; the PID control parameters can be changed on the DDC. The operational

[3]The DHS receives a 0–10 V set point signal mapped to a minimum and maximum temperature on the secondary side of 20 °C and 80 °C, respectively.

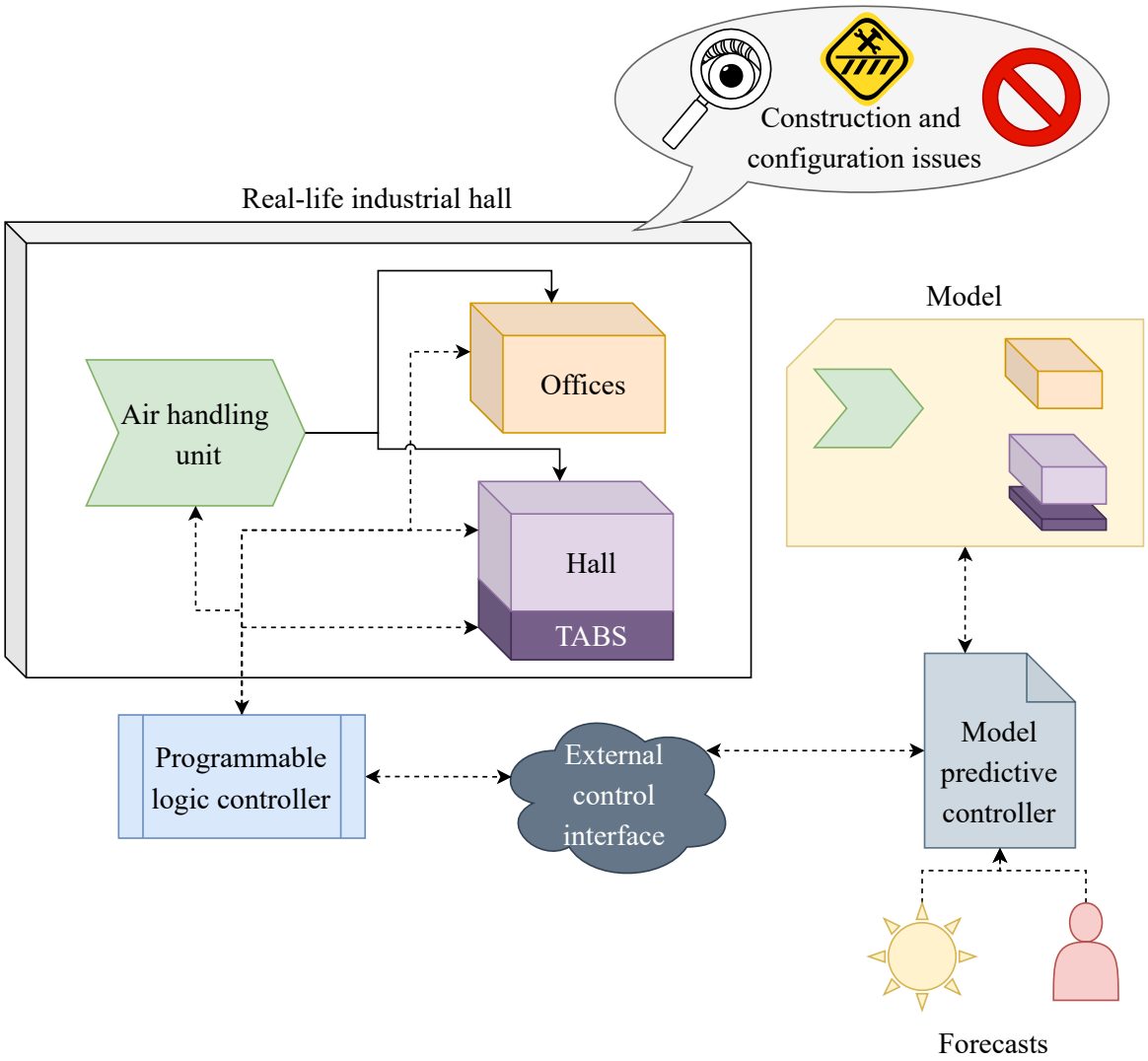

Figure 3 – Conceptualization of the case study.

limit of 55 °C is set as well on the DDC for the primary return water temperature, at which it will stop supply immediately.

Air Handling Unit Figure 2 shows the schematic structure of the AHU. In normal operation, all flaps of the AHU are opened 100 %. Additionally, the fans are controlled to match the required SUP. In this example control, the required SUP is a fixed value for hall 1 of 6500 m^3/h and a fixed value for the individual parts of the office area, concretely 150 m^3/h per office room, 240 m^3/h for each of the conference rooms and 200 m^3/h for each bathroom, resulting in a total of 7830 m^3/h. As no air is exhausted to the outside aside from the AHU, the ETA fan is set to the same volume flow rate. In practice, the fan control is given by a power fraction of the fan speed. Therefore, the speed signal is determined via a PID controller for each fan according to the actual and set volume flow rate.

According to Figure 2, the AHU offers two heating coils, a heat recovery (HR), a cooling coil, and a steam humidifier (SH) to condition the SUP, however, there are no sensors for temperature/humidity within the plant but only on the four connections to the external system, e.g. outdoor air (ODA), SUP, ETA and exhaust air (EHA). Within the AHU, the preheater (PH) and the subsequent frost protection sensor are located before the HR. Without a temperature sensor behind the PH, to avoid the frost protection triggering, an esti-

mated temperature behind the PH is used which serves as a virtual data point for this measurement in the following energy balance 1 and 2. All equations are noted in continuous form.

$$T_{\text{PH,water,supply,set}} = \frac{\dot{Q}}{\dot{m}_{\text{water}} \cdot c_{\text{p,water}}} + T_{\text{PH,water,return}} \tag{1}$$

$$\dot{Q} = \max\{\dot{m}_{\text{air}} \cdot c_{\text{p,water}} \cdot (T_{\text{air,min}} - T_{\text{ODA}}) + X_{\text{air}} \cdot c_{\text{p,vapour}} \cdot (T_{\text{air,min}} - T_{\text{ODA}})), 0\} \tag{2}$$

In this equation, $T_{\text{air,min}}$ is the minimum air temperature, which should be reached after the PH if the ODA temperature drops too low. Its value is set to 8 °C for safety so that the HR will still have the potential to recover heat with a temperature difference of $(T_{\text{ETA}} - T_{\text{air,min}}) \approx 12\,\text{K}$. The mass fraction of water in the air X_{air} is calculated by using the Antoine equation:

$$X_{\text{air}} = 0.622 \cdot \frac{p_{\text{vapour,sat}}}{\frac{p_{\text{air}}}{\phi} - p_{\text{vapour,sat}}} \tag{3}$$

$$p_{\text{vapour,sat}} = 611.657 \cdot e^{17.2799 - \frac{4102.99}{T_{\text{ODA}} - 35.719}} \tag{4}$$

Since the heat cannot be transferred with a temperature difference of 0 K between the water and air side, the temperature set point is adjusted by a fixed temperature difference:

$$T_{\text{PH,water,supply,set}} = \frac{\dot{Q}}{\dot{m}_{\text{water}} \cdot c_{\text{p,water}}} + T_{\text{PH,water,return}} + T_{\text{delta,HEX}} \tag{5}$$

Whenever possible, the HR should be active to save energy. One exception occurs, if the ETA temperature is higher than the SUP temperature set point and the ODA temperature is not too much lower. In this case, the HR can overshoot the temperature set point on SUP side, especially with the additional heat generated by the fan operation. Proper management of the bypass is not considered in this exemplary control; here, the bypass is set to be fully opened. As in the EHA, a condensate drip tray is installed, another exception is a summer case in which hot, moist ODA is cooled down by the ETA and condensation occurs within the SUP where no condensation drip tray is installed. In the HR control, again, no sensor for the humidity is available and a virtual data point for the estimated relative humidity is calculated according to the following equation:

$$\phi_{\text{HR,estim.}} = \frac{p_{\text{air}}}{p_{\text{vapour,sat}} \cdot (1 + \frac{0.622}{X_{\text{air}}})} \tag{6}$$

Again, the saturation pressure and mass fraction of water in the air is calculated using the Antoine equation (see equations (3) and (4)). Is the estimated relative humidity after the HR system above 90 %, the bypass is opened to bypass the HR and thus avoid condensation. Additionally, the temperature after the HR system is not measured as well and hence an estimated temperature is calculated for its virtual data point:

$$\begin{aligned} T_{\text{HR,out,estim.}} &= (T_{\text{ETA}} - T_{\text{ODA}}) \cdot \eta_{\text{HR}} + T_{\text{ODA}} \\ &\forall\, T_{\text{ODA}} \geq 8 \\ T_{\text{HR,out,estim.}} &= (T_{\text{ETA}} - T_{\text{ODA}}) \cdot \eta_{\text{HR}} + 8 \\ &\text{otherwise.} \end{aligned} \tag{7}$$

This estimated temperature is used within the reheater (RH) control, since the RH shall provide the remaining heat to reach the SUP set point. The control of the RH is based on the strategy presented in [43], where the valve opening, as well as the pump speed, is controlled by a two-step PID control. This leads to an improved control quality and less energy consumption of the pump compared to a standard control strategy, where only the valve opening is manipulated and the pump runs at a constant speed. However, the control strategy requires speed variable pumps, additional temperature information on the air side, and the design points for the set point calculations.

Due to a short mixing distance, an operation of the SH was avoided with the current configura-

tion. The corresponding issues are described in section 3.1.

Thermally active building system The TABS is controlled via a PID control using the supply water temperature set point and its actual temperature and generating a signal for the mixing valve. A system limitation of maximum 50 °C was given by the constructor, just to avoid a surface ground temperature above 27.5 °C. The supply water temperature set point is determined by a heating curve using the mean ambient air temperature and following the equation

$$T_{\text{water,supply,set}} = T_{\text{air,amb.,mean}} \cdot m + n \qquad (8)$$

where m is the slope and n the offset. The parameters are -1.0 for the slope and 35 °C for the offset. The TABS is turned into an off-mode when the ambient air temperature exceeds 15 °C.

Ceiling Panel Heaters As the CLGs consist of two hydraulic circuits, one admixing, and one throttling circuit, both circuits are controlled individually: First, the admixing circuit is controlled just as the TABS providing a supply water temperature according to an ambient-air-coupled heating curve with parameters -1.481 for the slope and 52 °C for the offset. The throttling circuit utilizes a PID control for the heating power according to the room temperature where the set point is given by a fixed value of 20.5 °C with a user-adjustable offset of ±5 °C via potentiometer. The actual room temperature is provided by a radiation sensor. Similar to the TABS, the CLGs are turned off when the ambient air temperature exceeds 15 °C.

Ceiling Induction Diffusers On the central heat distributor, the CIDs' admixing circuit also includes a PID control with the supply temperature set point resulting from a heating curve with parameters -1.0 for the slope and 45 °C for the offset. The throttling circuit, which is located directly at the CIDs, is controlled by the zone controllers, the exact control routine is unknown.[4] As for the cooling side, the implementation will be similar, while the control has to consider condensation on the outside of the insulation or within the cooled air. As the DCS does not work more efficiently with a higher return water temperature, the supply set point will be set to a fixed value of 12 °C for the PID control of its admixing circuit while the corresponding throttling circuit is controlled by the zone controller.

Battery and Bathroom Ventilation As no set point was given for the ventilation rate or the volume flow for the battery ventilation, both fans are set to 65 % of the nominal speed resulting in a constant volume flow rate of 234 m^3/h. This set point was chosen due to acoustic reasons. The same set point is given for the bathroom ventilation.

Jet Nozzles and Extract Air The JNs offer the possibility to adjust their outlet angle as well as the volume flow through each nozzle. To avoid draft, the angle is settable by a potentiometer allowing for absolute angles between 0 and 60° downwards. For the volume flow, again, a fixed set point is used dividing the nominal volume flow rate of hall 1 by the number of outlets. In this case, each jet nozzle receives a set point of 650 m^3/h. The set point for the ETA in hall 1 corresponds to the SUP in hall 1 and is distributed over two volume flow controllers. While the JNs do support reheating and recooling by external heat exchangers, there is no sensor to check the resulting temperature and humidity. So far no model has been implemented to calculate these virtual data points, hence, in the baseline control, the external heat exchangers for the JNs have been neglected.

Ambient Air The mean ambient temperature for the heating curves is derived by a 12 h average

[4] However, this control routine is PID-based as well and the PID control parameters can be adjusted via web interface

of the ODA temperature, which was taken from the AHU. The calculation works with several arrays of average values to save storage and which are consecutively updated for 1 s, 1 min, 1 h, and 12 h.

2.4.2 Model-Predictive Control

To test the applicability of advanced control methods to improve the building operation, an MPC problem is defined and applied to the BACS in a case study. As described in the previous section, the baseline control has no supervisory routine, meaning all subsystems will operate individually but are not coordinated[5]. From our experience, this is quite common, in particular, if no proper commissioning management is applied and each operator is just responsible for their own plant. Hence, the subsequent sections cover a simplified MPC formulation to function as supervisory control and coordinate heat demand and generation of the subsystems, and learnings to consider in future implementations.

Requirements The foremost concern to solve in modern buildings is the practical applicability of MPC. In the literature, the modeling effort is regularly reported to be a major challenge [21]. As our intention merely lies in displaying the functionality, this issue is addressed by applying a supervisory MPC based on simplified models that can be created with limited effort. Note that this approach drastically reduces the model accuracy and hence the suitability of MPC as mentioned by da Silva et al. [28]. A comprehensive evaluation would have to consider and estimate the implementation effort as well and compare it with the operational benefits [20]. In this regard, maintenance of the control may also play an important role [20]. On the other hand, building documentation is often incomplete, which makes the creation of a comprehensive system model very challenging. To compensate this effect, in the case study, instead of creating a comprehensive model for the entire system, rather small subsystem models are used in a distributed MPC. Not only does this approach reduce the complexity of the single models but it also allows to use different model formulations and modeling software in different subsystems, compare [44]. By that, the level of detail can be adjusted appropriately for each sub-model.

Energy saving potential of the case study As the hall and the office area offer reheating and recooling possibilities by decentralized heat exchangers before the JNs and within the CIDs, respectively, situations in which the AHU is in heating mode and the majority of the supplied zones are in cooling mode, must be avoided to achieve high overall energy efficiency. Moreover, the TABS with its comparatively high inertia may supply heat to the hall 1 while the AHU and the decentralized heat exchangers in the hall are in cooling mode. Therefore, a proper alignment of TABS and ventilation system should be pursued, compare [45].

Further potential for energy saving results from the consideration of occupation times. In unoccupied times, the heating mode temperature set points should be lower and the cooling mode set points should be higher than during occupation. Furthermore, the ventilation rate could be reduced. The role of the control algorithm is to determine a suitable time before the beginning and the end of the occupied period, respectively, to adapt the operation to the approaching change of boundary conditions.

Demand of the hall zone The zones' demands are considered by minimizing the temperature deviations between the actual temperatures of the ETAact air T_{ETA} and the respective set points $T_{\mathrm{hall,set}}$. Note that the actual system merely offers two temperature measurements indicating the actual room temperature of the hall 1: One measurement is located in a room control unit

[5] The subsystems often refer to the ambient air as an overall reference and demand supply is managed by user input via offsets, the generation is not sufficiently affected though.

at one side of the hall, and the other one is the ETA measurement in the AHU. The ETA temperature is a combined temperature for hall 1 and the office area, however, the greater share - roughly 83 % - belongs to the hall 1 ETA. During the occupation, the operator sets the hall air temperature set point directly. During unoccupied times, the only requirement is that the actual hall air temperature must not fall below 15 °C.

Demand of the office zone In the offices, the offset position of the room thermostat Δ at a given room temperature T_{office} is used to derive the current SUP temperature the occupant wishes to receive. This implicit demand is obtained using fuzzy inference [46]. It transforms the two states, namely measured room temperature and position of the thermostat into so-called crisp set point values for the SUP. The required linguistic rule base is thus created using skfuzzy[6]. One example of a rule is: "if the room temperature is very high and the thermostat position is very low, the desired SUP temperature should be very low". Using the so-called fuzzy membership functions, the linguistic rule base is transformed into a characteristic field. The advantage of this approach is the intuitive and comparatively simple creation of rules while still achieving a rather complex two-dimensional characteristic field. A visualization of the obtained characteristic field is included in figure 4.

Optimization problem The optimization problem is defined in equation (9) and constraints (10) to (14). The cost function J is determined to minimize the Energy consumption, represented by the energy flows $\dot{E}_i$ and a waited term for the discomfort represented by the temperature difference between set and actual temperature.

$$\begin{aligned} \text{minimize } J = & \int_{t_1}^{t_2} \sum_{i=1}^{n} \dot{E}_i \, \mathrm{d}t \\ & + b \cdot \left(T_{\text{hall}}(t_2) - T_{\text{hall, set}}\right)^2 \end{aligned} \tag{9}$$

$$\text{s. t.}$$

$$E_i = f_i(u_i, w_i, x_i) \tag{10}$$

$$\dot{x}_i = 0 \tag{11}$$

$$T_{\text{hall}} = C x_{\text{hall}} \tag{12}$$

$$\dot{x}_{\text{hall}} = A x_{\text{hall}} + B_u u_{\text{hall}} + B_w w_{\text{hall}} \tag{13}$$

$$u_{\text{min}} \leq u_i \leq u_{\text{max}} \tag{14}$$

where n is the number of energy consumers

- Hall heat exchanger
- Office heat exchanger
- TABS
- AHU

u, w and x are the control inputs, the disturbances, and the state variables of the ith consumer, respectively. T_{hall} and $T_{\text{hall, set}}$ are hall air temperature and hall temperature set point, respectively. E_i is the energy consumption of the ith consumer. The weighting factor b of the quadratic penalty term $T_{\text{hall}}(t_2) - T_{\text{hall, set}}$ is chosen such that the term is in the same order of magnitude as the energy consumption if a deviation of 1 K between set point and actual temperature occurs.

All systems are modeled as linear time invariant (LTI) systems. Due to the high inertia of the thermo-hydraulic systems, it is assumed that the consumers are always in a steady state, i.e. $\dot{x}_i = 0$. The subsystems, their manipulated variables, and disturbances are depicted in Figure 5. These are the set point of the AHU SUP temperature $T_{\text{SUP,set}}$ and the set point of the TABS supply water temperature $T_{\text{TABS,set}}$. Moreover, in each zone, the SUP can be heated or cooled by a PID-controlled heat exchanger. In the hall, the maximum achievable temperature difference is assumed to be constrained to the range [-3, 3]. In the offices, the maximum temperature difference is in the range [-10, 10].

[6] https://pythonhosted.org/scikit-fuzzy

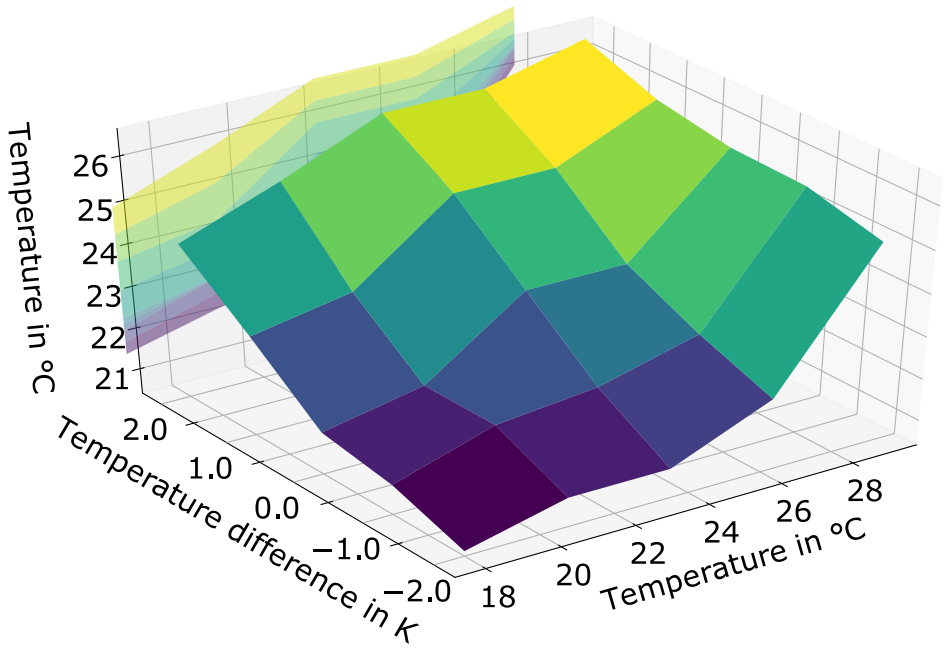

Figure 4 – Visualization of the fuzzy rule base (created with skfuzzy) used to determine the SUP temperature set point in the case study

The energy consumption of each consumer is a function f of the manipulated variables and the disturbances associated with this consumer. The energy consumption of the AHU is given in equation (15)

$$E_{\text{AHU}} = \dot{m} c_p \cdot \big[T_{\text{SUP}} - \big(T_{\text{ETA}} \cdot \eta_{\text{HR}} + T_{\text{ODA}} \cdot (1 - \eta_{\text{HR}})\big)\big] dt \tag{15}$$

where $\dot{m}$ is the mass flow rate, c_p is the specific heat capacity at constant pressure, T is the temperature, and η_{HR} is the heat recovery efficiency that is assumed to be constant at $70\,\%$.

The ETA temperature results from the mixture of all air flows according to equation (16).

$$T_{\text{ETA}} = \frac{1}{\dot{m}} \cdot \sum_i \dot{m}_i \cdot T_{\text{ETA, i}} \tag{16}$$

The energy consumption of the office and the hall heat exchangers is given in equation (17) and (18)

$$E_{\text{office}} = \rho \cdot \dot{V}_{\text{office}} \cdot c_p \cdot (T_{\text{SUP}} - T_{\text{SET, office}}) dt \tag{17}$$

$$E_{\text{hall}} = \rho \cdot \dot{V}_{\text{hall}} \cdot c_p \cdot (T_{\text{SUP}} - T_{\text{SET, hall}}) dt \tag{18}$$

where $\dot{V}$ is the air volume flow rate and ρ is the air density.

For evaluating the control quality, the root mean squared error (RMSE) is used (compare [47]).

The following paragraph describes the distributed scheme used to solve the optimization problem. In this approach, each subsystem optimization is supposed to deliver a scalar cost value.

Distributed MPC The optimization problem is solved in a distributed manner. Distributed algorithms perform subsystem optimizations while considering the interactions between the subsystems [48]. The experimental hall contains various subsystems that influence each other. These physical interactions can be expressed as coupling variables. For instance, the AHU SUP temperature couples the various zones. In previous works, a distributed control algorithm has been developed that requires a limited amount of system knowledge [49]. Accordingly, in this paper, the algorithm has been extended to suit the requirements of the experimental hall operation. The basic approach is to solve subsystem optimization problems for discrete values of the coupling variables that are assumed constant during

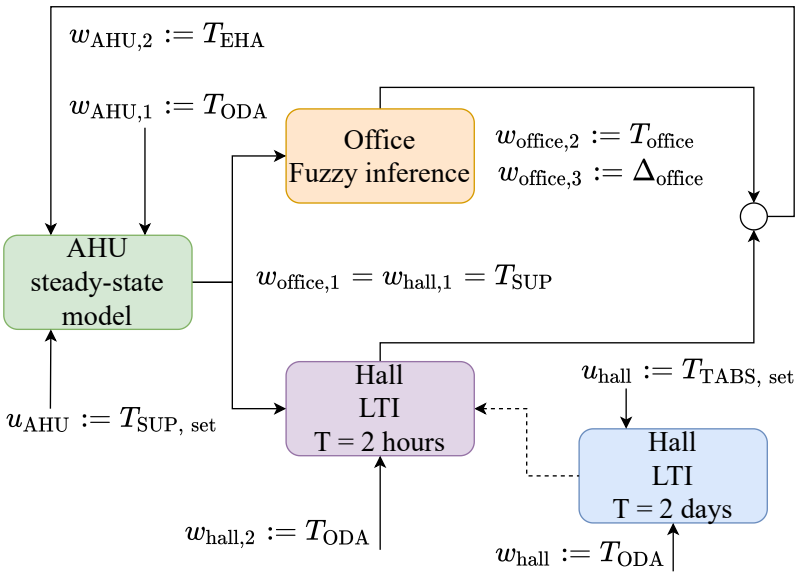

Figure 5 – Overview of subsystems, their manipulated variables, and disturbances

the entire prediction horizon. The results of the optimization are stored in tables, comparable to state-action tables used in Q-Learning [50]. These tables are provided to subsystems that are located upstream in direction of the main flow coupling the subsystems. For reasons of simplicity, only the steady-state outputs of the subsystem predictions are considered. The predictions are based on a one-step prediction horizon, i.e. the control input is constant for the entire horizon length T. All code including the models presented in the following is available on GitHub[7].

Time horizons The optimization of the hall subsystem is divided into two optimizations to consider the fact that the system is composed of subsystems with different inertia. One optimization over a horizon length of two days aimed at determining the TABS set point, which generally shows slow dynamics due to the high mass of the system. An additional optimization with a horizon length of 2 hours is used for the remaining air-based systems to determine the SUP temperature. Both optimizations use an hourly prediction of the outdoor temperature. Figure 5 provides an overview of subsystem variables and prediction horizons.

[7] https://github.com/RWTH-EBC/pyDMPC

Modeling A basic model of the hall 1 is created in the modeling language Modelica® using the open source library AixLib [51] and especially the resistor-capacitor (RC) models as presented in [52]. By contrast, in the offices, only the fuzzy inference engine is used to determine the SUP temperature set point.

The RC models of the hall have the advantage of good interpretability compared to e. g. neural networks. Moreover, they can be used in optimization problems that can be solved very efficiently by many available solvers. The equivalent electric circuit diagram of the hall is shown in Figure 6. The RC model contains the following four capacities:

- air (C_{air})
- inner walls ($C_{1\mathrm{i}}$)
- outer walls ($C_{1\mathrm{o}}$)
- floor. ($C_{1\mathrm{f}}$)

Furthermore, to model the environment and the TABS supply, two temperature sources are inserted. Both temperature sources are connected to the rest of the system via a resistance ($R_{\mathrm{rest,\,o}}$ and $R_{\mathrm{rest,\,f}}$). The air capacity is connected to three resistances that allow heat flux from the

- outer walls ($R_{1\mathrm{o}}$)
- inner walls ($R_{1\mathrm{i}}$)
- floor. ($R_{1\mathrm{f}}$)

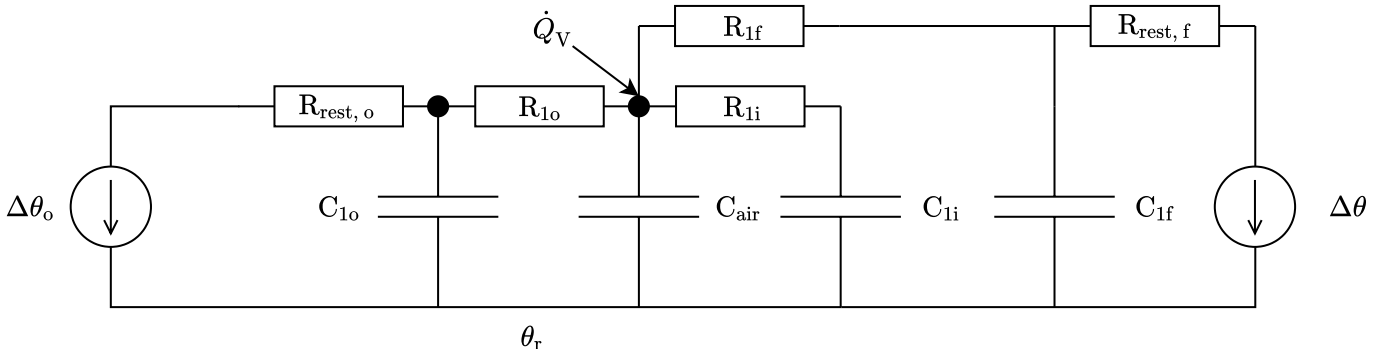

Figure 6 – Electric circuit representing the resistance-capacity model of the hall in the case study.

The ventilation of the hall is modeled as an ideal mass flow source, ideal mixture of the hall air, and equality of supply and ETA volume flow rates. This air exchange corresponds to an equivalent heat flux as depicted in figure 6.

The MPC operation is compared with the baseline operation in section 3.2.

2.5 Monitoring and Commissioning

To identify issues with the BACS, in addition to some commissioning procedures, monitoring, and simulation were used.

2.5.1 General BACS Commissioning

The general commissioning process that was applied is divided into different stages:

1. Complete plants like the DHS are commissioned individually (see 2.5.3).
2. All actuators are tested for their signal transmission by sending a set point and observing the response either visually or with a designated sensor data point.
3. Sensors are tested by inducing a state change, observing the respective change, and evaluating if the observation was meaningful.
4. Controls are tested by either coupling them with simulation models (see 2.5.2) or deploying the control directly to the system and carefully observing the system behavior via monitoring data.

While the PID-based example control solely relies on the ambient air temperature as the central coupling element, no advanced supervisory control was implemented which omits even more elaborate commissioning of the system. Therefore, the proposed baseline control represents a case in which the plants' control has been commissioned individually, which is quite common and especially does not fully cover all operational states nor does it make use of the full potential aligning set points among different plants as described in section 2.4.2 [53]. Note, that this procedure requires expert knowledge and a structured thorough approach to decide whether a reaction is considered meaningful or not. In case of a failure, the solution is rather individual and based on observation and expert knowledge again.

2.5.2 Simulation and Commissioning of TABS

To avoid cracks in the concrete due to expansion at high temperature gradients, a heat-up phase for the TABS had to be conducted. In the first step of the heat-up phase, the temperature of the concrete was measured and the inflow temperature of the TABS was set 5 K above the measured concrete temperature. This temperature was kept for seven days. Afterwards, the temperature has been increased 5 K each day until an inflow temperature of 50 °C was reached (compare Figure 8). The code for the heat-up phase is implemented in the automation program. To

test the functionality of the program and the correct temperature increase a priori, we set up a simulation model of the TABS and the hydraulic circuit in the modeling language Modelica®. The model includes all control-relevant temperature sensors and actuators, such as pump and valve, and is connected via an ADS interface to the control program. In this way, the automation program could be tested in a software-in-the-loop environment without the risk of damaging the TABS (see Figure 7).

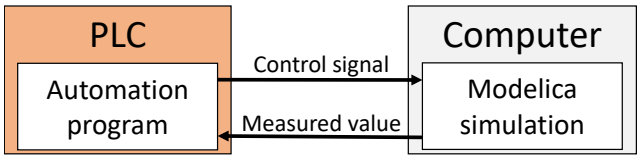

Figure 7 – Setup of the Software-in-the-loop test of the automation program.

2.5.3 Commissioning of DHS

The DHS was tendered and delivered by an external company. As such, this company was responsible for the commissioning. To run the commissioning procedure for the DHS, a heat consumer is required, which demands a noticeable share of the total provided power. As the CLG and TABS were prepared for their commissioning, they were used as consumers for the DHS commissioning.

The technician set a preconfigured control and chose the related PID control parameters and time constants according to his experience. A few set points were tested and the supply water temperature on the secondary side was observed during this process via an analog display.

2.5.4 Monitoring

Monitoring supports visualization, interpretation, and association of data. Two monitoring approaches support the commissioning process: Natively, the PLC offers the possibility to create lists of variables and watch their state in a live view. This is especially used for the control commissioning as the current mode and state of all variables can be read directly in the live mode allowing for a logical linear check of the functionality. Additionally, the monitoring is enhanced by data transmission to a cloud server and visualization in a Grafana® dashboard. Data visualization offers a quick overview of semantically-related data points and trending while the cloud service provides features such as alerting to notify on hazardous or unwanted operational conditions. Figure 9 depicts an example of the dashboard visualization. In this figure, the set points of TABS supply water and CLG supply water are followed satisfactorily well by their actual temperatures.

3 Results and Discussion

3.1 Detected issues

In this section, during the commissioning detected issues are described. More specifically, the method used for detecting the issue, the significance and relevance as well as the solution are presented.

3.1.1 District heating station

On the DHS, two issues were discovered during the commissioning procedures described in 2.5.3 and 2.5.2. The DHS includes two valves for controlling its power: a high load valve that is specified with a high volume flow and therefore destined for coarse control and a low load valve for fine-tuning. During a low-load operation, the valve actuators were detected to be installed the wrong way around. This caused the DHS to control the high load valve for the low load operation, whereby it could not control the desired temperature on the secondary side sufficiently.

The issue was solved by switching the valves implying moderate to high expenses and delaying the commissioning of all downstream systems. Another issue was detected during the

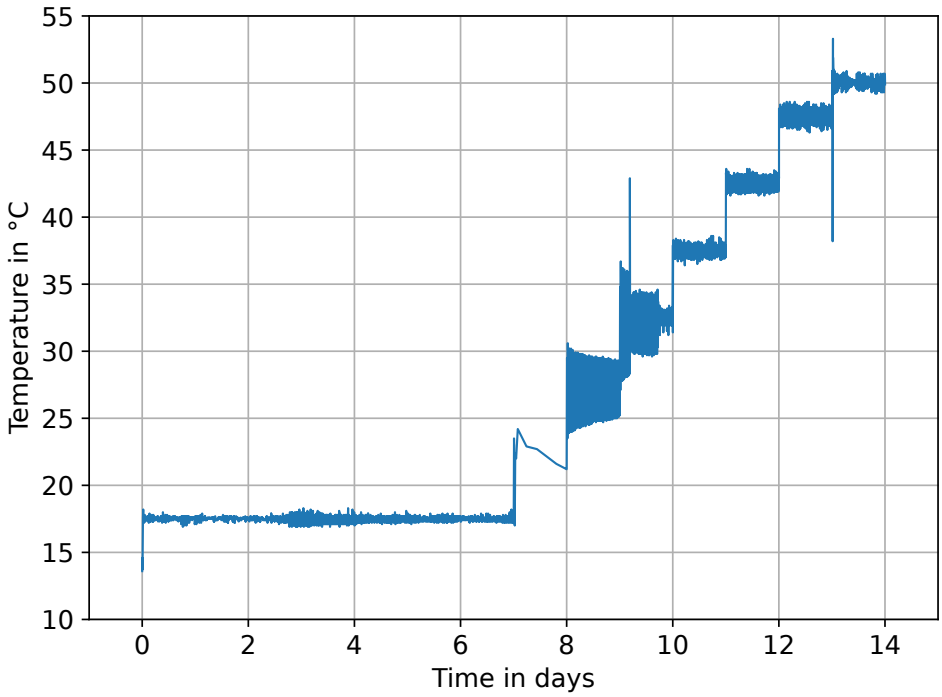

Figure 8 – Temperature curve of the commissioning procedure of the TABS

TABS commissioning by observing the primary supply temperature. This temperature showed a scattering of roughly 20 K even though the supply water temperature set point did not vary during this process. Therefore, we assumed the PID control of the DHS to be poorly parameterized. As a consequence, we reduced the proportional gain of the PID controller leading to reduced oscillations of approx. 10 K. With this spread, the downstream mixing circuit that supplies the TABS could reduce the oscillations conclusively to roughly 2 K (see figure 8). Besides a reduced control quality, oscillating behavior causes more component strain and leads to increased energy consumption [54].

Due to our experience, the commissioning differs from the actual operation, since different loads, occupation, weather conditions etc. are usually not considered. Similarly, it seems common that the technician chooses control parameters based on their experience, since they do not know in detail the interaction with the rest of the system and can only rely on their experience with different installations. Therefore, we conclude the probability of suboptimal parameterization to be rather high. In principal, adjusting the parameters requires just a few inputs, however, finding a set of proper parameters might require a deeper analysis and thus higher effort.

3.1.2 3-way-mixing valves

Admixing circuits based on 3-way-valves support two configurations:

1. The 3-way-valve is positioned in the supply water flow and functions as a mixing valve.
2. The 3-way-valve is positioned in the return water flow and functions as a distribution valve.

Figure 10 depicts a view of the different configurations. The 3-way-valve supports three openings, whereat for no load, e. g. 0 % relative valve opening, and full load, e.g. 100 % relative valve opening, one gate is completely blocked. During normal operation, the closed side and the open side next to it travel between gates A and B partially allowing flow from both gates A and B and resulting in a mixture of hot supply water from the distributor and cooled return water from the

Figure 9 – Monitoring dashboard visualizing data points of the JNs, TABS and CLGs.

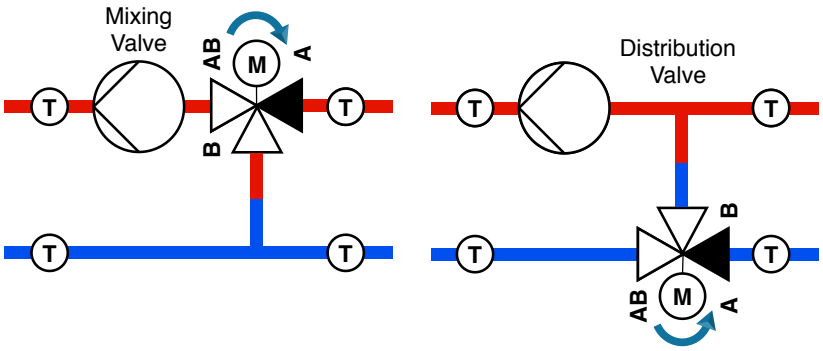

Figure 10 – Schematic view of an admixing circuit with 3-way-valve in both mixing and distributing configuration; the filled triangle of the valve marks the blocked opening

consumer. In both cases, for no load, path A to the distributor is blocked. Under full load, no return water should be mixed, which requires the openings to move according to the posed direction in Figure 10 so that path B through the bypass is blocked. Note the different directions of the motion for the different configurations, e. g. for the mixing valve in Figure 10, the closed opening travels clockwise while for the distribution valve, the movement is counterclockwise. The function is checked by the observation of a combination of temperatures and the pump operation.

To solve a faulty positioning, the construction has to be rebuilt and the valve repositioned. These types of constructional errors fully impede the functioning and have consequently a high impact on the energy efficiency. In this case, the movement of the free opening was adjusted to comply with Figure 10. Considering the wrong valve positioning on the DHS, we conclude constructional errors to occur frequently. The causes lie among other things in deadline pressure, e.g. leaving the installer with less time to check the installation properly, and the sequential construction process and non-uniform/non-central data filing, e.g. leading to outdated plans. As this issue required a constructional change in the piping system, it was rather elaborate and should be avoided by checking the labeling and

execution planning more carefully during the installation phase.

3.1.3 Temperature probes

On the heat distributor, each system's supply flow offers a temperature measurement. As the distances on the distributor are rather short, these should technically show the same value for the primary supply temperature. However, they were observed to display severely different measurement values varying up to 3 K deviation. Therefore, all temperature probes on the distributor were then checked against a fixed temperature sensor at different temperature levels using a portable temperature calibration bath[8], and the calibration curves were obtained.

At this point, the procedure was rather elaborate, since the PT100 temperature sensors had no cable length reserved on the distributor side, and removing the probes from their thermowells was difficult due to their accessibility. Additionally, the calibration bath merely offered space to check 2 probes at the same time at maximum and required to stabilize its temperature which took a decent amount of time. Depending on the number of temperature calibration points, e. g. [55] recommends at least 3, and the number of probes, the process can take several days.

The calibration curves could then be provided to the PLC as user-defined offset and gain to the IO values. Even though the 3-wire temperature probes have 1/3 DIN accuracy, the deviations were quite significant.[9] Temperature probes are one of the most common devices in BES installations (compare the list of devices in the supplementary material), which increases the chances of inaccuracies occurring among them. However, PID control is based on temperature differences and hence not as much dependent on the actual temperature reference. Besides this, wherever set points are provided by user preference like a given offset indicating "too warm" or "too cold", the exact temperature is not necessarily useful at all which is taken advantage of in the fuzzy logic described in section 2.4.2. If considered, the calibration should be carried out before installation. For the given accuracy class and 3-wire configuration, the cost difference between PT100 and PT1000 is not much noticeable. The higher resistance of PT1000 makes them much more robust against measurement inaccuracies due to cable length. Therefore, for new installations, it is recommended to use PT1000 over PT100 temperature probes. However, the effect of imprecise temperature data on user comfort or on control behavior has yet to be analyzed in more detail. As no specific issues or user complaints were found to be present in the uncalibrated system, we currently expect no significant issues, thus, suggesting waiving an extensive calibration.

[8] LR-CAL Fluid 100-N

[9] The average deviation accounts for 1.38 K, the standard deviation amounts to 1.31 K over all measurements.

3.1.4 BACS function and maintenance

In the process of programming the example control for the case study, we experienced that a fragmented and non-standardized control software implementation is error-prone and along with the wrong BES component installation one of the main reasons why systems lack functionality or do not achieve their desired efficiency. Even though the IEC 61131 does provide some guidelines, the code structure and concrete implementation is an individual task and comes down to the experience of the automation engineer or programmer. Thus, we estimate the occurrence of errors in this process to be very high, especially considering the complexity of larger systems and, again, deadline pressure. In [56], we addressed this issue by developing a code library to reduce the amount of individual programming required.

In this particular case, we faced our PLC stopped working due to programming errors. The issues could be narrowed down to the BACnet® implementation, however, because code was executed in different parts of the function blocks and on different levels, the program was too hard to maintain and the issue could not be fixed. Even if

the error was fixed, the program still would have been difficult to maintain. For this reason, the automation software was completely rewritten from scratch. Although the mode-based structure and the object-oriented programming were used in the previous version as well, the programming now follows a much more linear and standardized structure, where code is exclusively executed within the corresponding methods of a class. Besides this, all process results are stored within properties, and values are merely transferred between classes via property exchange. Following this approach, the program became more robust and easier to maintain, as one can easily travel in live mode from one to the next method to see which method is executed. Rewriting the software cost a lot of time and should be avoided by proper preparation and proactive planning in earlier stages as well as following a clearly defined structure and programming standard.

3.1.5 AHU

For the ambient air temperature calculation, the ODA temperature data point from the AHU was used, as described in section 2.4.1. Hence, the mean ambient air temperature, which is used for all heating curves, is directly coupled with the AHU functionality. Furthermore, the AHU features a frost protection mode overwriting the local control: In this mode, the ventilators are stopped, all flaps closed and both heaters are operated at 100 % causing the temperature in the first chamber to raise and therefore influence the air temperature measurement. As the temperature will rise above 50 °C, the heating curves will force all corresponding systems to cool or turn off instead of heating. Assuming a 24/7 operation, under normal operational circumstances, the frost protection mode should not be active at any time. When applying scheduling, the AHU would require a special starting routine to smoothly turn from frost protection mode to normal operation mode. Otherwise, the dynamic of the ODA temperature cannot follow the temperature of the frost protection sensor causing the control to intervene too late. The issue could simply be tackled with a separate temperature sensor before the air handling unit in the ODA section or by fetching the temperature from a designated weather server.

Another issue was detected lately, where the heat recovery was found active while the ODA temperature was below the extract air temperature and the SUP temperature set point overshoot. This special case had not been addressed before but had been active for a while because the building could not properly cool down without additional cooling. Therefore, the control implementation has been adjusted to the one described in section 2.4.1, which especially helped to cool at night.

One visually significant issue was detected by rust formation on the AHU floor right before the SUP outlet. Space restrictions within the building resulted in a short length requirement for the whole AHU. Therefore, due to a very short distance between the steam distributor of the SH and the subsequent filter, the steam air mixture is incomplete. As a consequence, following the vortex flow of the fan, a moist unmixed share hits the filter in the center inducing condensation within the filter elements and on the frame's edges. The issue resulted from a combination of the strict space requirements, a lack of experience and insufficient communication in the planning stage. Nowadays, there are more tools available supporting the planning and indicating errors in the configuration more clearly, reducing the probability of comparable issues. An approach to calculate the required distance is, for instance, given by Nordmann Engineering [57]. Furthermore, many applications, e. g. in schools or office buildings, might not have specific humidity requirements, thus omitting the necessity of integrating humidification. To avoid further pollution of the filter and rust formation, the operation was stopped; operation of < 20 % relative humidity are relatively rare and no further specific requirements were given. A possible technical solution might be adjusting the air flow by

adding guiding elements and slightly adjusting the steam distribution which was suggested by a simulation.

Another visually conspicuous issue was the PH being clogged by dust and particles. Since the PH is installed on an upper part of the AHU, however, this issue was detected rather accidentally by randomly opening the corresponding chamber. Another method to detect this issue could be a trend observation of the supply fan pressure, as this increases with a larger amount of clogging. When the PH builds up higher pressure losses, the fan power would rise to achieve the same volume flow but induces higher noise emissions and energy consumption. This issue is a classic maintenance task. The PH was cleaned and will be checked periodically.

3.1.6 Modbus®

The JN and ETA control are connected via the serial Modbus® RTU protocol. Unlike the broadcast functionality in the BACnet® protocol, Modbus® clients require a request from the master and return the corresponding information to the master. Since Modbus® RTU does not feature multi-master functionality, only one client can be operated at the same time and all the communication has to be initiated and finished by the master. This requires the automation software to care about the time the request and answer process takes and to operate all devices in serial. Besides this, Modbus® does not define one specific physical layer according to the OSI model.[10] Hence, each vendor follows a different convention regarding namings and internal signal processing. This becomes especially complex when bias and termination have to be considered as well. Therefore, it took several attempts to get the cabling correct and working.

[10] The Modbus® organization recommends using the EIA/TIA-485 standard, however, several options are given (see https://www.modbus.org/docs/Modbus_over_serial_line_V1_02.pdf chapter 3), which lead to vendors using differing denotations referring to the OSI model like TxD/RxD (see https://www.janitza.de/kommunikation-ueber-die-rs485-schnittstelle.html)

3.2 Comparison between MPC and baseline control

This section covers the results of the case study. In the following, the results of the modeling and optimization of the experimental hall operation are presented.

Calibration The results of the manually tuned model of the hall are depicted in Figure 11. The tuning included monitored time series data with a duration of one month. The most relevant inputs are ODA temperature, the TABS supply temperature, and the AHU SUP temperature. The influence of solar irradiation and events such as the opening of the gates in the hall is neglected. Further uncertainties are related to the building orientation, the actual outside conditions, estimated heat transfer coefficients, and further unconsidered loads in the operation. The model uncertainty can thus be considered rather high. However, additional tuning would imply additional effort while the intention was neither to optimize the accuracy nor the ratio of benefits to expenses, but to demonstrate one example MPC to work with the given limitations. To account for the uncertainty, the model has been tuned such that it rather underestimates the actual temperature. With this model tuning, the MPC is expected to result in heat flow rates that may be slightly too high, which is preferable over an insufficient heat flow rate. Still, with a root mean squared error of 0.59 K and similar dynamic behavior, the model can be considered a suitable approximation for MPC.

Simulation setup Before applying the MPC to the real system, a simulation case study is conducted. In this simulation, the plant model is similar to the real-life building. The air volume flow rates are the same as in the case study in section 2.4. The office temperature and the thermostat position are varied using Modelica® step function generators. The resulting SUP temperature set point which is inferred by the fuzzy logic

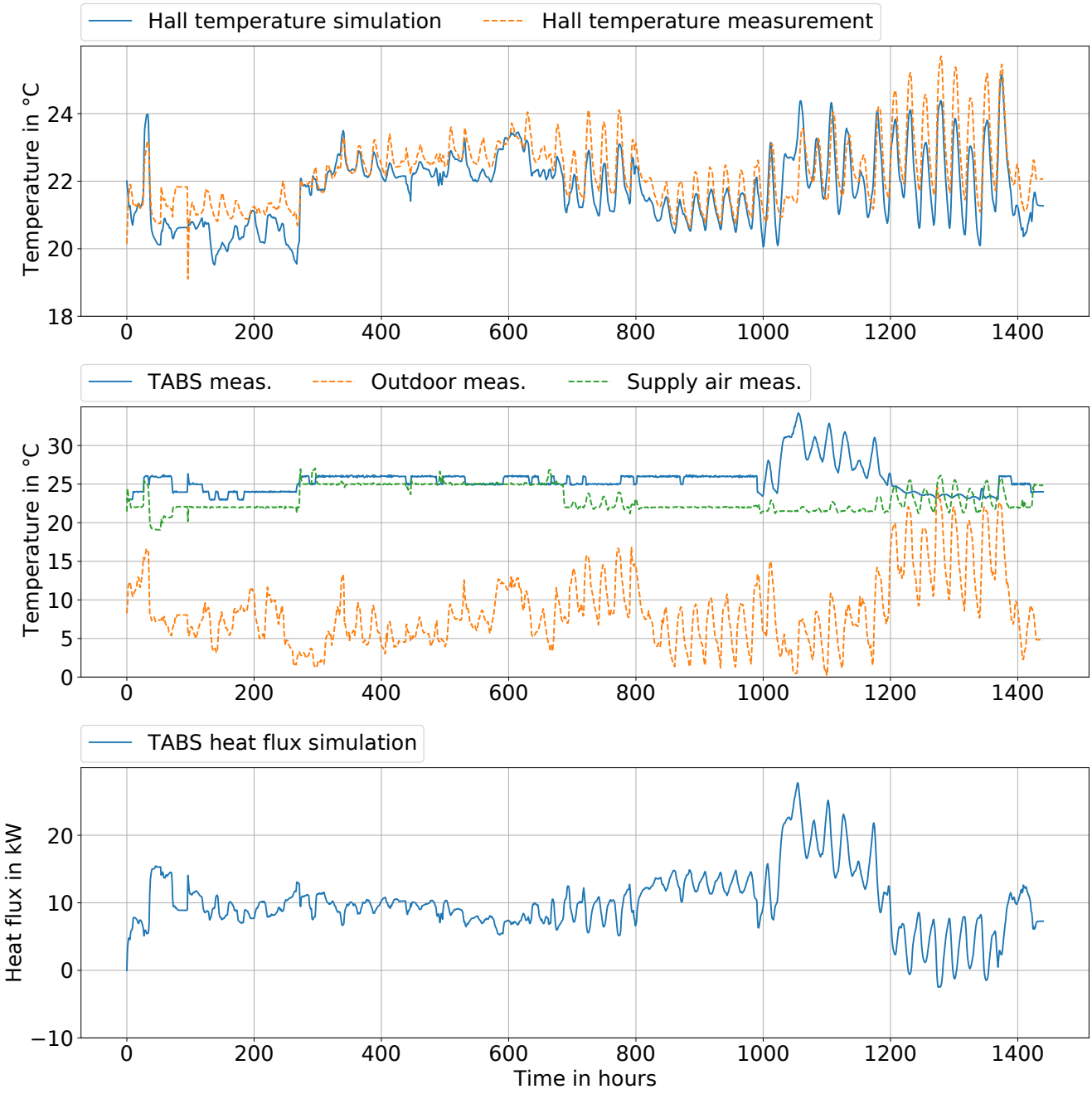

Figure 11 – Results of a calibration of an RC model of the hall; top: simulated and measured air temperatures in the hall; middle: temperatures of the TABS, the AHU and the outdoor temperature; bottom: resulting TABS heat flux.

controller as described in section 2.4.2, is depicted in Figure 12.

Benchmark strategy To benchmark the performance of the MPC algorithm, a very basic benchmark strategy is applied that, during the two simulated days, consists of a constant SUP temperature set point of 25 °C and a TABS supply temperature set point determined using the moving average of the past 24 hours of the outdoor temperature and the heating curve according to equation (8). As with the example controls, this benchmark does not claim to serve as a general reference scenario but rather a baseline for comparison. Further research is necessary to develop

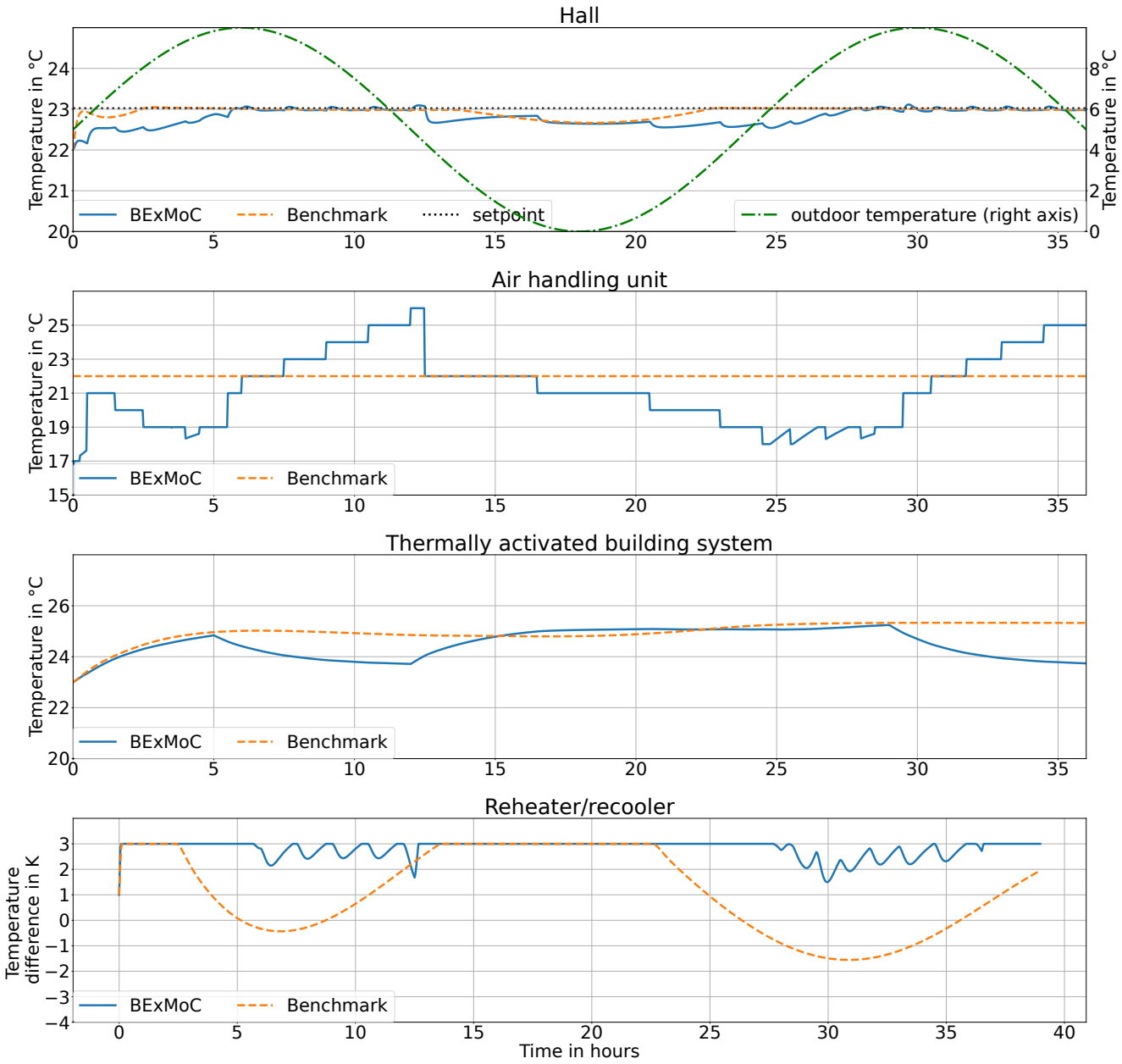

Figure 12 – Results of a simulation case study; top: SUP temperature set points demanded in the offices and actual SUP temperature provided by the AHU; middle: hall air temperature set point and actual air temperatures in the hall as achieved by the studied control algorithm and the benchmark strategy; bottom: TABS temperatures generated by the studied control algorithm and the benchmark strategy.

and agree on a general state-of-the-art reference control. However, in practice, BACS still often rely on rather basic control as the MCT budget is too small and investors save their money by leaving out functionalities. In the following, we refer to the benchmark strategy as the benchmark and the MPC algorithm as the algorithm.

Simulation results In Figure 12, the actual temperatures in the hall zone are depicted, both for the algorithm and the benchmark scenario. With a RMSE of 0.28 K, the control quality in the algorithm scenario is slightly lower than the quality in the benchmark scenario (RMSE of 0.13 K), as it deviates from the set point more often. The algorithm varies the AHU SUP temperature fre-

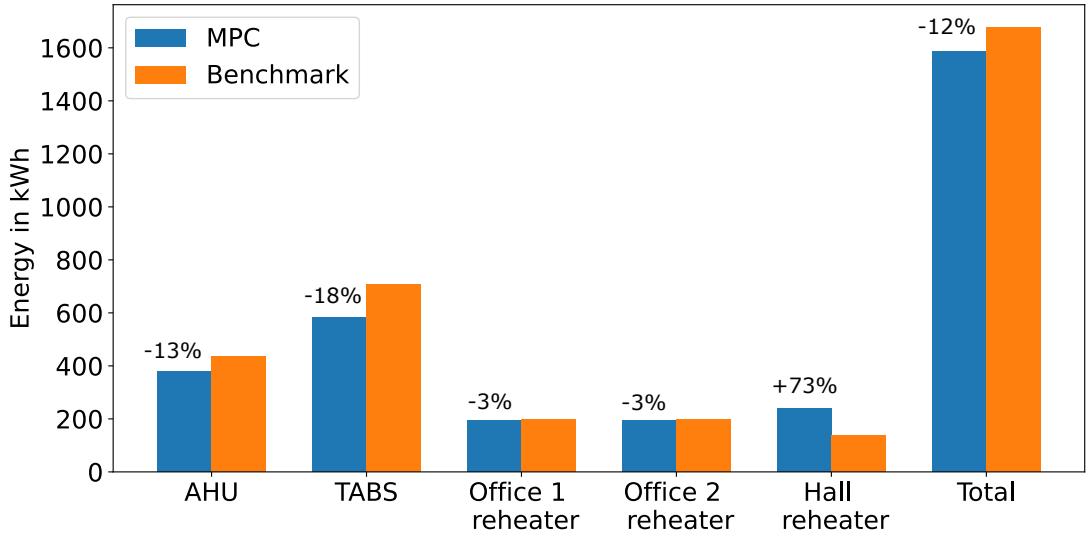

Figure 13 – Energy consumption of the components in the hall in the case study achieved by the studied control algorithm and a benchmark strategy.

quently, which is plausible to find a trade-off between the demands of the different zones. The temperature difference over the heat exchanger of the hall is mostly close to the upper limit in the algorithm scenario. By contrast, in the benchmark scenario, the temperature is partly negative, which means that the heat exchanger cools the supply air, thus dissipating energy supplied to the air flow in the air handling unit. The algorithm keeps the temperature of the TABS supply water slightly lower or equal to the value of the benchmark.

To compare the energy consumed by the different components, Figure 13 shows the distribution and also reveals that the algorithm saves approximately 12 % final energy. The savings result mainly from the lower consumption of the AHU and TABS, which is partly compensated by the higher consumption of the reheater in the hall. It shall also be noted that a small part of the savings must be attributed to the fact that the average hall temperature achieved by the algorithm is 0.12 K lower than the temperature achieved by the benchmark strategy, leading to lower transmission losses.

Real-life experiment setup In the real-life case study, only the hall zone is considered as the HVAC system had not been completed by the time we conducted the experiments presented in the following. The ETA temperature measured in the AHU is used as a proxy for the actual temperature in the hall. Similar to the simulation case study, the TABS supply temperature set point and the AHU SUP temperature set point are to be determined. Additionally, in this case, study, the occupation times are considered as well. The occupied period is the same on each day, from 6 am to 6 pm. During the unoccupied times, the algorithm may choose any set point above 15 °C. The outdoor temperature is plotted in Figure 14. It is in the range of 10 to 25 °C.

Real-life experiment results As Figure 14 shows, the algorithm chooses a low SUP temperature set point a couple of hours before the end of the occupied period. Conversely, it increases the set point 4-5 hours before the beginning of the occupied period. The TABS supply, indicating that the model and the weather forecast never indicated a significant demand.

The algorithm shows the expected behavior and achieves temperatures in the hall that are close to the set point. Deviations may have occurred due to undetected events such as the opening of the gates of the hall which can also influence the

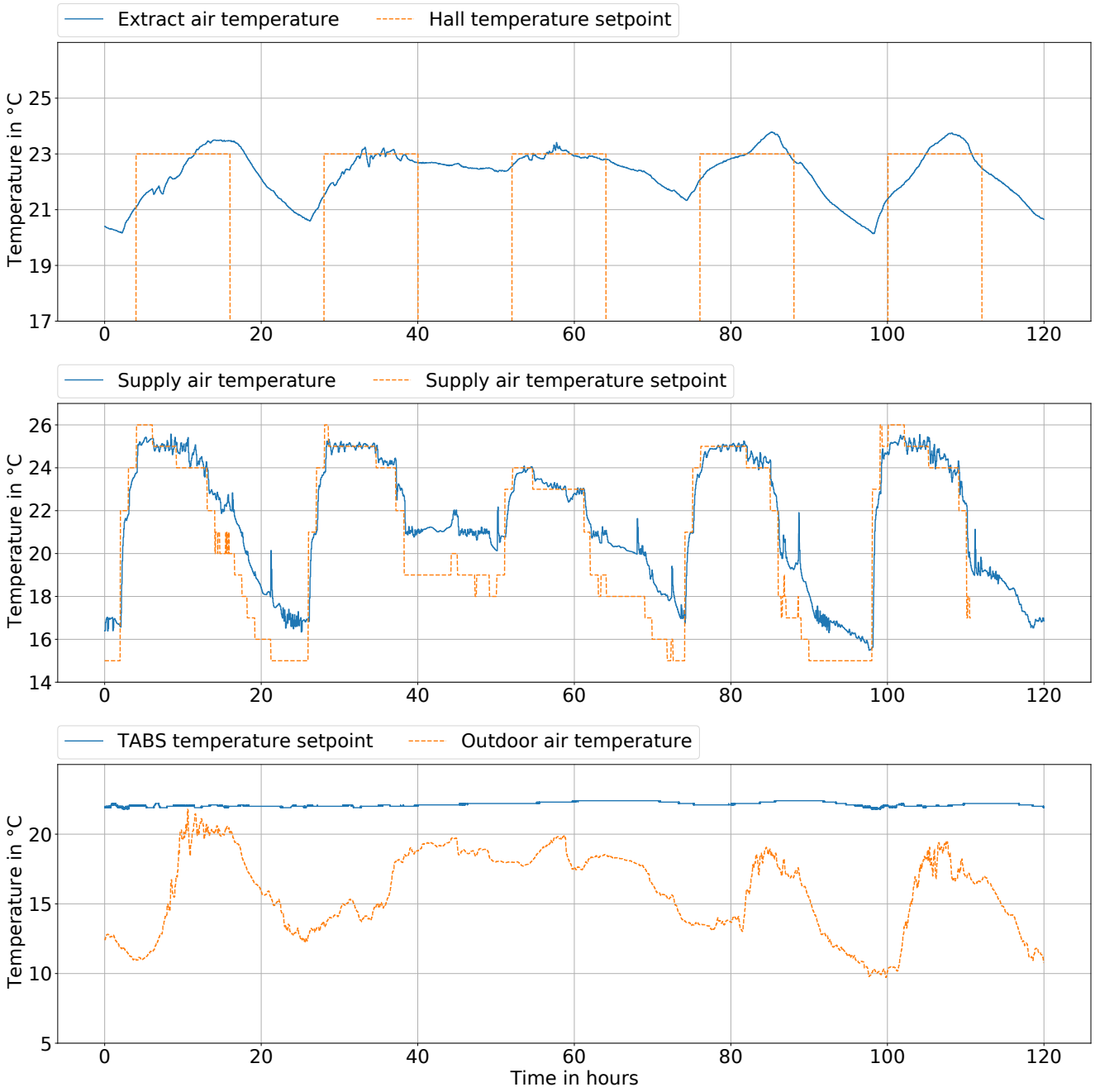

Figure 14 – Results of a real-life case study; top: air temperature set point and actual air temperature in the hall; middle: SUP temperature set point and actual SUP temperature in the hall; bottom: TABS supply water temperature and outdoor temperature.

thermal balance of the hall. The omission of solar radiation in the model is another factor that could drive the plant-model mismatch.

Discussion Based on the results obtained so far, we conclude that the applied MPC algorithm achieves a good trade-off between implementation effort and control performance. There are many uncertainties involved that are mitigated by the distributed architecture that allows using various types of models depending on the degree of uncertainty in the various subsystems. In the simulation study, the comparison showed the improvement potential compared to the benchmark strategy that included typical set

points for the system. By varying the set points, the MPC algorithm avoided simultaneous heating and cooling. In the real-life experiment, we showed that the implementation in the experimental hall is feasible and that plausible actions are taken. The test hall itself showed potential for being used as a test bench in the future. A prerequisite is the installation of the DCS, which will allow performing the same experiment in the real-life building as it was performed in the simulation case study.

4 Conclusion

In this work, we presented the application of a model-predictive control (MPC) in a building automation and control system (BACS) and figured out challenges for the practical implementation and commissioning. To demonstrate the functionality and usability, both a proportional-integral-derivative (PID)-based example control and an MPC were developed and compared in a case study in the proposed system. As many approaches exist but they are rarely validated in practice, special focus was laid on the estimation and evaluation of obstacles that occurred during the implementation and application process.

The building energy system (BES) utilized for the experimental study can be classified as a representative heating, ventilation and air conditioning (HVAC) system accompanied by typical additional heating systems like a thermally active building system (TABS). As such, a major contribution is a comprehensive BES and HVAC description supported by detailed supplementary material, which can be used for the creation and calibration of building and BES models. A comparably detailed building, BES and model identification description, for instance, is found in Žáčeková et al. [22], however, they do not go into detail about the measurement and control technology (MCT) communication and data acquisition. Nevertheless, they do also report issues - in this case related to the measurement accuracy - to be found in the real building. This supports our findings of the temperature sensors showing severe deviations, which may lead to reduced performance of advanced control methods.

Another focus of this study was laid on sharing experiences, especially in the construction and commissioning phase. Here, table 2 summarizes the issues of which most of these can be traced back to a lack of experience supporting the results in [33]. However, following the described commissioning procedures in section 2.5 could help identifying these kind of issues before they affect the energy performance.

Furthermore, from the experienced issues, we derive the following lessons learned:

- 3-way-valves require thorough examination for their flow and spindle movement before installation
- For better maintainability of programmable logic controller (PLC) code, we recommend transferring variables between different function blocks solely by properties and code execution only within methods (strict object-oriented approach)
- Usage of PT1000 over PT100, random sample examination of the measurement accuracy, omission of elaborate calibration
- Usage of an individual sensor for the ambient air conditions
- Missing sensor data - to some extent - can be compensated by calculating virtual data points

The proposed MPC has not been focused on tuning it to maximum efficiency but rather on showing its functionality and limitations. It uses a distributed approach which allows for an individual implementation and hence a detailed degree for each part of the system, which can help to find a good trade-off between the modeling effort of the subsystems and the expected benefits. Moreover, the modeling effort can be considered rather low as a simplified linear time invariant (LTI) model was used for the main part of the system, while the other part was approximated using fuzzy logic. The LTI model was tuned manually and validated using measurement data from

Table 2 – Summary of discovered issues

Issue	Impact on energy efficiency and costs	Probability of occurrence	Fixing effort
Constructional errors (especially valve positioning)	high	high	high
Automation software architecture / maintainability	very high	high	very high
Bus protocol specialties	high	high	high
Temperature elements accuracy	low	medium	high
Steam humidifier air mixture length	low	low	high
Vendor control parameters / configuration	medium	high	low-medium
Coupled control data points	high	low	low
Special operational cases	low	medium	medium
(No sensor / data point available	medium	medium	varies)

the real BACS and even with the given uncertainties and simplifications, the MPC simulated the measurement data fairly well with a root mean squared error (RMSE) of 0.59 K and a comparable dynamic behavior. Despite the lower modeling effort compared to other studies in the literature, the algorithm performed better than the benchmark strategy.

Similarly, the PID-based example control may not be a general reference. Further research is required to 1) develop a general reference control, 2) develop a sophisticated evaluation method and the related key performance indicators and 3) develop a fair and structured evaluation routine since performance boosts will still heavily rely on the ambient conditions. Hence, future studies should focus on making different control approaches comparable by developing standard key performance indicators and agreeing on a reference control as a benchmark. However, the proposed BACS offers a lot more research opportunities: For instance, investigations in fault detection and diagnosis, training of machine learning algorithms with the generated data, data-driven control approaches, automated commissioning or evaluation and improvement of model accuracy as well as automated model-generation approaches. Another future aspect will be enhancing the BACS by full Internet-of-Things capabilities to further investigate in new technologies and their suitability in combination with classic BACS' components.

Supplementary Material

This section covers a description of the related supplementary material provided with this paper:

- The file "17-08-28_EON Versuchshalle_1-50 _Grundrisse, Schnitte, Ansichten.dxb" contains the floor plan of the industrial hall.
- The file "ADSDataPoints.xlsx" contains a list of PLC datapoints and a short explanation. Note that of these only data points with the "ADS" suffix can communicate with external systems, e. g. such as the MPC, via the automation device specification (ADS) inter-

face. Data points using the ADS interface only support one way of communication, so either being writable or readable but not both at the same time.
- The file “CoolingScheme.drawio” contains the cooling scheme in editable format.
- The file “HeatingScheme.drawio” contains the heating scheme in editable format.
- The file “HeatingScheme.pdf” contains the heating scheme in non-editable format.
- The file “ListOfDevices.xlsx” contains a full list of devices and associated data points (number of analog or digital/binary inputs and outputs). Two sheets are available where the devices are sorted by location or by system.
- The file “MCT Schema.vsdx” contains the MCT scheme in editable format.
- The file “MCT Schema.pdf” contains the MCT scheme in non-editable format.
- The files with “.ifc” filename extension contain the different partial models of the building information model (BIM). “ModelTesthall_EBC Stahlgeruest.ifc” covers the positioning of steel beams for collision detection. “ModelTesthall_EBC Umbau EG.ifc” represents the hydraulic installations supplying the HVAC system on the ground floor. “ModelTesthall_Fernkälteanlage OG.ifc” and “ModelTesthall_Fernwärmeanlage OG.ifc” include the hydraulic installations of the district cooling station (DCS) and district heating station (DHS), respectively. “ModelTesthall_Fernkälteanlage OG.ifc” is a ring circuit in hall 1 supplying test facilities with cold water from one of the DCS. “ModelTesthall_Fernwärmerohre.ifc” covers the supplying pipes from DHS to the ceiling panel heater (CLG) in hall 2. “ModelTesthall_KabelKanal_OG.ifc” inlcudes a cable tray from the MCT cabinet to the DCS and DHS. Finally, “ModelTesthall_Klimaanlage_EG.ifc” and “ModelTesthall_Klimaanlage_OG.ifc” contain the air duct system and air handling unit (AHU) for ground floor and first floor, respectively.
- Data presented in this study is contained in the separate data folder.

The supplementary material is openly available at https://github.com/RWTH-EBC/EBC-SupplementaryMaterials.

Acknowledgment

We would like to thank the TROX GmbH for their contribution with ventilation components. Further thanks to our electrical and mechanical workshop who contributed to a large share of the installations. This research was funded by the European Regional Development Fund (ERDF) grant number EFRE-0800527, KEU-1-006A and the Federal Ministry for Economic Affairs and Climate Action (BMWK) grant number 03EI6051A. The funders had no role in the design of the study; in the collection, analyses, or interpretation of data; in the writing of the manuscript; or in the decision to publish the results.

Nomenclature

Abbreviations

The following abbreviations are used in this manuscript:

ADS	automation device specification
AHU	air handling unit
amb.	ambient
BACS	building automation and control system
BES	building energy system
BIM	building information model
CID	ceiling induction diffuser
CLG	ceiling panel heater
DCS	district cooling station
DDC	direct digital controller
DHS	district heating station
EBC	Institute for Energy Efficient Buildings and Indoor Climate
EHA	exhaust air
estim.	estimated
ETA	extract air
HEX	heat exchanger
HR	heat recovery
HVAC	heating, ventilation and air conditioning
JN	jet nozzle
LTI	linear time invariant
MCT	measurement and control technology
MPC	model-predictive control
ODA	outdoor air
OSI	Open Systems Interconnection
out	outlet
PH	preheater
PID	proportional-integral-derivative
PLC	programmable logic controller
RAS	room automation system
RC	Resistor-Capacitor
RH	reheater
RMSE	root mean squared error
sat	saturated
SET/set	set point
SH	steam humidifier
SUP	supply air
TABS	thermally active building system

TBE	technical building equipment
VFC	volume flow controller

Symbols

The following symbols and measurement units are used in this manuscript:

η	efficiency	$\%$ or -
ϕ	relative humidity	$\%$ or -
ρ	air density	$\mathrm{kg/m^3}$
A	linear state space system matrix	various
b	weighting factor	$\mathrm{J/K}$
B	linear state space system matrix	various
c_p	specific heat capacity at constant pressure	$\mathrm{J/(kg\,K)}$
C	linear state space system matrix	various
E	energy	J
m	slope of a heating curve	-
$\dot{m}$	mass flow	$\mathrm{kg/s}$
n	offset of a heating curve	°C
p	pressure	Pa
$\dot{Q}$	heat output	W
R	thermal resistance	$\mathrm{K/W}$
t	time	s
T	temperature	°C or K
$\Delta\Theta$	temperature difference	K
u	control input	various
$\dot{V}$	air volume flow rate	$\mathrm{m^3}$
w	disturbance	various
x	state variable	various
X	mass fraction of water in the air	$\mathrm{g/kg}$

References

[1] Thibaut Abergel, Brian Dean, and John Dulac. "Towards a zero-emission, efficient, and resilient buildings and construction sector: Global Status Report 2017". In: *UN Environment and International Energy Agency: Paris, France* (2017).

[2] Xiaodong Cao, Xilei Dai, and Junjie Liu. "Building energy-consumption status worldwide and the state-of-the-art technologies for zero-energy buildings during the past decade". In: *Energy and Buildings* 128 (2016), pp. 198–213. ISSN: 0378-7788. DOI: 10.1016/j.enbuild.2016.06.089.

[3] Liu Yang, Haiyan Yan, and Joseph C. Lam. "Thermal comfort and building energy consumption implications – A review". In: *Applied Energy* 115 (2014), pp. 164–173. ISSN: 0306-2619. DOI: 10.1016/j.apenergy.2013.10.062.

[4] Wooyoung Jung and Farrokh Jazizadeh. "Human-in-the-loop HVAC operations: A quantitative review on occupancy, comfort, and energy-efficiency dimensions". In: *Applied Energy* 239 (2019), pp. 1471–1508. ISSN: 0306-2619. DOI: 10.1016/j.apenergy.2019.01.070.

[5] Ghezlane Halhoul Merabet et al. "Intelligent building control systems for thermal comfort and energy-efficiency: A systematic review of artificial intelligence-assisted techniques". In: *Renewable and Sustainable Energy Reviews* 144 (2021), p. 110969. ISSN: 1364-0321. DOI: 10.1016/j.rser.2021.110969.

[6] Pervez Hameed Shaikh et al. "A review on optimized control systems for building energy and comfort management of smart sustainable buildings". In: *Renewable and Sustainable Energy Reviews* 34 (2014), pp. 409–429. ISSN: 1364-0321. DOI: 10.1016/j.rser.2014.03.027.

[7] K. J. Chua et al. "Achieving better energy-efficient air conditioning – A review of technologies and strategies". In: *Applied Energy* 104 (2013), pp. 87–104. ISSN: 0306-2619. DOI: 10.1016/j.apenergy.2012.10.037.

[8] D. Mariano-Hernández et al. "A review of strategies for building energy management system: Model predictive control, demand side management, optimization, and fault detect & diagnosis". In: *Journal of Building Engineering* 33 (2021), p. 101692. ISSN: 2352-7102. DOI: 10.1016/j.jobe.2020.101692.

[9] Mariantonieta Gutierrez Soto and Hojjat Adeli. "Recent advances in control algorithms for smart structures and machines". In: *Expert Systems* 34.2 (2017), e12205. ISSN: 0266-4720. DOI: 10.1111/exsy.12205.

[10] Mostafa Abdel-Geliel, F. Qaud, and H. A. Ashour. "Realization of adaptable PID controller within an industrial automated system". In: *11th IEEE International Conference on Control & Automation (ICCA)*. IEEE, 18/06/2014 - 20/06/2014, pp. 965–970. ISBN: 978-1-4799-2837-8. DOI: 10.1109/ICCA.2014.6871052.

[11] Abdul Afram and Farrokh Janabi-Sharifi. "Theory and applications of HVAC control systems – A review of model predictive control (MPC)". In: *Building and Environment* 72 (2014), pp. 343–355. ISSN: 0360-1323. DOI: 10.1016/j.buildenv.2013.11.016.

[12] Gianni Bianchini et al. "An integrated model predictive control approach for optimal HVAC and energy storage operation in large-scale buildings". In: *Applied Energy* 240 (2019), pp. 327–340. ISSN: 0306-2619. DOI: 10.1016/j.apenergy.2019.01.187.

[13] Petru-Daniel Moroşan et al. "A distributed MPC strategy based on Benders' decomposition applied to multi-source multi-zone temperature regulation". In: *Journal of Process Control* 21.5 (2011), pp. 729–737. ISSN: 0959-1524. DOI: 10.1016/j.jprocont.2010.12.002.

[14] Diana Manjarres et al. "An energy-efficient predictive control for HVAC systems applied to tertiary buildings based on regression techniques". In: *Energy and Buildings*

152 (2017), pp. 409–417. ISSN: 0378-7788. DOI: 10.1016/j.enbuild.2017.07.056.

[15] Roozbeh Sangi and Dirk Müller. "A novel hybrid agent-based model predictive control for advanced building energy systems". In: *Energy Conversion and Management* 178 (2018), pp. 415–427. ISSN: 0196-8904. DOI: 10.1016/j.enconman.2018.08.111.

[16] Anjukan Kathirgamanathan et al. "Data-driven Predictive Control for Unlocking Building Energy Flexibility: A Review". In: *Renewable and Sustainable Energy Reviews* 135 (2021), p. 110120. ISSN: 1364-0321. DOI: 10.1016/j.rser.2020.110120. URL: http://arxiv.org/pdf/2007.14866v1.

[17] Thomas Schreiber et al. "Application of data-driven methods for energy system modelling demonstrated on an adaptive cooling supply system". In: *Energy* 230 (2021), p. 120894. ISSN: 0360-5442. DOI: 10.1016/j.energy.2021.120894.

[18] Christina Anastasiadi and Anastasios I. Dounis. "Co-simulation of fuzzy control in buildings and the HVAC system using BCVTB". In: *Advances in Building Energy Research* 12.2 (2018), pp. 195–216. ISSN: 1751-2549.

[19] Phillip Stoffel et al. "Evaluation of advanced control strategies for building energy systems". In: *Energy and Buildings* 280 (2023), p. 112709. ISSN: 0378-7788. DOI: 10.1016/j.enbuild.2022.112709.

[20] M. Killian and M. Kozek. "Ten questions concerning model predictive control for energy efficient buildings". In: *Building and Environment* 105 (2016), pp. 403–412. ISSN: 0360-1323. DOI: 10.1016/j.buildenv.2016.05.034.

[21] Gianluca Serale et al. "Model Predictive Control (MPC) for Enhancing Building and HVAC System Energy Efficiency: Problem Formulation, Applications and Opportunities". In: *Energies* 11.3 (2018), p. 631. DOI: 10.3390/en11030631.

[22] Eva Žáčeková, Zdeněk Váňa, and Jiří Cigler. "Towards the real-life implementation of MPC for an office building: Identification issues". In: *Applied Energy* 135 (2014), pp. 53–62. ISSN: 0306-2619. DOI: 10.1016/j.apenergy.2014.08.004.

[23] Roozbeh Sangi, Alexander Kümpel, and Dirk Müller. "Real-life implementation of a linear model predictive control in a building energy system". In: *Journal of Building Engineering* 22 (2019), pp. 451–463. ISSN: 2352-7102. DOI: 10.1016/j.jobe.2019.01.002.

[24] David Lindelöf et al. "Field tests of an adaptive, model-predictive heating controller for residential buildings". In: *Energy and Buildings* 99 (2015), pp. 292–302. ISSN: 0378-7788. DOI: 10.1016/j.enbuild.2015.04.029.

[25] Jie Cai et al. "A general multi-agent control approach for building energy system optimization". In: *Energy and Buildings* 127 (2016), pp. 337–351. ISSN: 0378-7788. DOI: 10.1016/j.enbuild.2016.05.040.

[26] Roel de Coninck and Lieve Helsen. "Practical implementation and evaluation of model predictive control for an office building in Brussels". In: *Energy and Buildings* 111 (2016), pp. 290–298. ISSN: 0378-7788. DOI: 10.1016/j.enbuild.2015.11.014.

[27] Alexander Kümpel et al. "A Representative Simulation Model for Benchmarking Building Control Strategies". In: *Proceedings of the 36th International Symposium on Automation and Robotics in Construction (ISARC)*. Ed. by Mohamed Al-Hussein. Proceedings of the International Symposium on Automation and Robotics in Construction (IAARC). International Association for Automation and Robotics in Construction (IAARC), 2019, pp. 242–249. DOI: 10.22260/ISARC2019/0033.

[28] Lucian Ribeiro da Silva, Rodolfo César Costa Flesch, and Julio Elias Normey-Rico. "Controlling industrial dead-time systems: When to use a PID or an advanced controller".

In: *ISA transactions* 99 (2020), pp. 339–350. DOI: 10.1016/j.isatra.2019.09.008.

[29] David Sturzenegger et al. "Model Predictive Climate Control of a Swiss Office Building: Implementation, Results, and Cost–Benefit Analysis". In: *IEEE Transactions on Control Systems Technology* 24.1 (2016), pp. 1–12. ISSN: 1063-6536. DOI: 10.1109/TCST.2015.2415411.

[30] Chin-Chi Cheng and Dasheng Lee. "Artificial Intelligence-Assisted Heating Ventilation and Air Conditioning Control and the Unmet Demand for Sensors: Part 1. Problem Formulation and the Hypothesis". In: *Sensors (Basel, Switzerland)* 19.5 (2019). DOI: 10.3390/s19051131.

[31] Pieter de Wilde. "The gap between predicted and measured energy performance of buildings: A framework for investigation". In: *Automation in Construction* 41 (2014), pp. 40–49. ISSN: 0926-5805. DOI: 10.1016/j.autcon.2014.02.009.

[32] Xing Shi et al. "Magnitude, Causes, and Solutions of the Performance Gap of Buildings: A Review". In: *Sustainability* 11.3 (2019), p. 937. DOI: 10.3390/su11030937.

[33] Christine Eon et al. "The Discrepancy between As-Built and As-Designed in Energy Efficient Buildings: A Rapid Review". In: *Sustainability* 12.16 (2020), p. 6372. DOI: 10.3390/su12166372.

[34] Patrick X.W. Zou et al. "Review of 10 years research on building energy performance gap: Life-cycle and stakeholder perspectives". In: *Energy and Buildings* 178 (2018), pp. 165–181. ISSN: 0378-7788. DOI: 10.1016/j.enbuild.2018.08.040.

[35] David James McElroy and Jan Rosenow. "Policy implications for the performance gap of low-carbon building technologies". In: *Building Research & Information* 47.5 (2019), pp. 611–623. ISSN: 0961-3218. DOI: 10.1080/09613218.2018.1469285.

[36] S. H. Lee and F.W.H. Yik. "A study on the energy penalty of various air-side system faults in buildings". In: *Energy and Buildings* 42.1 (2010), pp. 2–10. ISSN: 0378-7788. DOI: 10.1016/j.enbuild.2009.07.004.

[37] Zara Fahim and Xinlei Wang. "Improving the Energy Performance of a University Building through Fault Detection and Building Systems Diagnostics (CH-12-C020)". In: vol. 118. 2012.

[38] Burak Gunay et al. "Energy and comfort performance benefits of early detection of building sensor and actuator faults". In: *Building Services Engineering Research and Technology* 39.6 (2018), pp. 652–666. ISSN: 0143-6244. DOI: 10.1177/0143624418769264.

[39] Pedro Domingues et al. "Building automation systems: Concepts and technology review". In: *Computer Standards & Interfaces* 45 (2016), pp. 1–12. ISSN: 0920-5489. DOI: 10.1016/j.csi.2015.11.005.

[40] mh-software GmbH. *mh-software*. URL: https://www.mh-software.de/ (visited on 02/01/2023).

[41] Yousaf Khalid. "Programmable logic controllers and Direct digital controls in Buildings". In: *Journal of Computing and Management Studies (JCMS)* (2018).

[42] Wolfgang Kastner et al. "Communication systems for building automation and control". In: *Proceedings of the IEEE* 93.6 (2005), pp. 1178–1203. ISSN: 0018-9219. DOI: 10.1109/JPROC.2005.849726.

[43] J. Teichmann et al. "Improving control quality and reducing pump energy consumption of AHU". In: *REHVA* (2018).

[44] Petru-Daniel Moroşan et al. "Building temperature regulation using a distributed model predictive control". In: *Energy and Buildings* 42.9 (2010), pp. 1445–1452. ISSN: 0378-7788. DOI: 10.1016/j.enbuild.2010.03.014.

[45] Jaewan Joe and Panagiota Karava. "A model predictive control strategy to optimize the performance of radiant floor heating and cooling systems in office buildings". In: *Applied Energy* 245 (2019), pp. 65–77. ISSN: 0306-2619. DOI: 10.1016/j.apenergy.2019.03.209.

[46] Varun Ojha, Ajith Abraham, and Václav Snášel. "Heuristic design of fuzzy inference systems: A review of three decades of research". In: *Engineering applications of artificial intelligence* 85 (2019), pp. 845–864. ISSN: 0952-1976. DOI: 10.1016/j.engappai.2019.08.010.

[47] Zheng O'Neill, Yanfei Li, and Keith Williams. "HVAC control loop performance assessment: A critical review (1587-RP)". In: *Science and Technology for the Built Environment* 23.4 (2017), pp. 619–636. ISSN: 2374-4731. DOI: 10.1080/23744731.2016.1239466.

[48] Walid Al–Gherwi, Hector Budman, and Ali Elkamel. "Robust distributed model predictive control: A review and recent developments". In: *The Canadian Journal of Chemical Engineering* 89.5 (2011), pp. 1176–1190. ISSN: 0008-4034. DOI: 10.1002/cjce.20555.

[49] Marc Baranski et al. "Comparative study of neighbor communication approaches for distributed model predictive control in building energy systems". In: *Energy* 182 (2019), pp. 840–851. ISSN: 0360-5442. DOI: 10.1016/j.energy.2019.06.037.

[50] M. Sridharan and G. Tesauro. "Multi-agent Q-learning and regression trees for automated pricing decisions". In: *Proceedings Fourth International Conference on MultiAgent Systems*. IEEE Comput. Soc, 10-12 July 2000, pp. 447–448. ISBN: 0-7695-0625-9. DOI: 10.1109/ICMAS.2000.858518.

[51] Dirk Müller et al. "AixLib - An Open-Source Modelica Library within the IEA-EBC Annex60 Framework". In: *Proceedings of the CESBP Central European Symposium on Building Physics and BauSIM 2016 : September 14-16, 2016, Dresden, Germany*. Stuttgart: Fraunhofer IRB Verlag, 2016, pp. 3–9. URL: https://publications.rwth-aachen.de/record/681852.

[52] M. Lauster et al. "Low order thermal network models for dynamic simulations of buildings on city district scale". In: *Building and Environment* 73 (2014), pp. 223–231. ISSN: 0360-1323. DOI: 10.1016/j.buildenv.2013.12.016.

[53] Fu Xiao and Shengwei Wang. "Progress and methodologies of lifecycle commissioning of HVAC systems to enhance building sustainability". In: *Renewable and Sustainable Energy Reviews* 13.5 (2009), pp. 1144–1149. ISSN: 1364-0321. DOI: 10.1016/j.rser.2008.03.006.

[54] Johannes Peter Fütterer. "Tuning of PID Controllers within Building Energy Systems". PhD thesis. Universitätsbibliothek der RWTH Aachen, 2018. DOI: 10.18154/RWTH-2017-10490.

[55] Mitglieder des Fachausschusses Temperatur und Feuchte des DKD in der Zeit von 2001 bis 2009. *Kalibrierung von Temperatur-Blockkalibratoren : Richtlinie DKD-R 5-4*. 2018. DOI: 10.7795/550.20180828AE.

[56] Markus Hans Schraven et al. "AixOCAT: Open-Source-Bibliothek für Automationssysteme". In: *atp Magazin* 9 (2019), pp. 48–51. ISSN: 2190-4111. URL: https://publications.rwth-aachen.de/record/768255.

[57] Nordmann Engineering AG. *Technische Planungs-Anleitung. Elektroden-Dampf-Luftbefeuchter*. URL: https://nordmann-engineering.com/wp-content/uploads/bulk-import/technische%20planungsanleitung_ohne%20DVR.pdf (visited on 03/02/2023).